UNIVERSIDADE FEDERAL DO ESPÍRITO SANTO

CENTRO DE CIÊNCIAS HUMANAS E NATURAIS

PROGRAMA DE PÓS-GRADUAÇÃO EM CIÊNCIAS BIOLÓGICAS

Molecular-based Phylogenetic Reconstruction of Pristocerinae (Hymenoptera, Bethylidae)

Daniele Ferreira Mugrabi

Vitória, ES
Abril, 2019

UNIVERSIDADE FEDERAL DO ESPÍRITO SANTO

CENTRO DE CIÊNCIAS HUMANAS E NATURAIS

PROGRAMA DE PÓS-GRADUAÇÃO EM CIÊNCIAS BIOLÓGICAS

Molecular-based Phylogenetic Reconstruction of Pristocerinae (Hymenoptera, Bethylidae)

Daniele Ferreira Mugrabi

Orientador: Celso Oliveira Azevedo

Tese submetida ao Programa de Pós-Graduação em Ciências Biológicas (Biologia Animal) da Universidade Federal do Espírito Santo como requisito parcial para a obtenção do grau de Doutora em Biologia Animal.

Vitória, ES
Abril, 2019

Dedico esta tese aos
meus amados filhos.

SUMÁRIO

Agradecimentos

Lista de tabelas

Lista de figuras

Apresentação 10

Resumo 12

Abstract 13

Capítulo I

1. Introduction 14

2. Materials and methods 15

Material selection and sorting 15

Extraction, amplification and DNA sequencing 16

Matrix of molecular data 17

Molecular phylogenetic analysis 17

Illustrations 18

Terminology and treatment 18

3. Results 18

4. Discussion 19

On double paramere 20

Other Bethylidae taxa 21

On apical projection of basiparamere 22

Clade B 22

Clade C 23

Clade D 24

Clade H and aedeagus divided into two rami (complex aedeagus) 27

On the morphology of complex aedeagus 28

Clade E 29

Clade F 31

5. Final Remarks 31

6. References 33

7. Tables and Figures 37

LISTA DE TABELAS

Table 1. Terminal taxa of phylogenetic analysis.

Table 2. Primer sequences (written 5’ to 3’) used and best models selected to the nine partitions obtained for the five molecular markers.

Table 3. Comparison between the morphological patterns found in *Acrenesia* large- and small-bodied styles.

LISTA DE FIGURAS

Figure 1. Maximum likelihood of Pristocerinae based on concatenated sequence data (COI, 28S, EF-1α, Pol II and LWRh). Values of bootstrap are given next to the branches.

Figure 2. Phylogenetic Bayesian reconstruction of Pristocerinae based on concatenated sequence data (COI, 28S, EF-1α, Pol II and LWRh). Values of posterior probability are shown next to the branches.

Figures 3–11. Male genitalia. 3–5. *Caloapenesia* in lateral view. 5. Sclerite of aedeagus basis (e) in dorsal view. 6–7. *Calobrachium*. 6. Lateral view. 7. Dorsal view. 8–10. *Pseudisobrachium*. 8. Lateral view. 9. Dorsal view. Internal view of basiparamere. 11. *Eupsenella* in lateral view. Label: (va) ventral arm of paramere; (da) dorsal arm of paramere; (pb) projection dorsal and basal of basiparamere covering the base of aedeagus. Scale bar: 100 µm, except 7 (20 µm) and 11 (50 µm).

Figures 12–20. Male genitalia. 12–14. *Heterocoelia* in dorsal view. 15–16. *Zimancus* in dorsal view. 17–18. *Apenesia* in dorsal view. 19. *Parascleroderma* in lateral-dorsal view. 20. *Foenobethylus* in dorsal view. Label: (pb) projection dorsal and basal of basiparamere covering the base of aedeagus; (va) vental arm of paramere; (da) dorsal arm of paramere; (p) apical projection of the basiparamere; (al) laleral and apical lobe of aedeagus; (ca) central area of of aedeagus. Scale bar: 100 µm.

Figures 21–29. Male genitalia. 21. *Foenobethylus* in vetral view. 22–29. Lateral view of complex aedeagus. 22–23. *Pristepyris*. 22. External lateral face 23. Internal lateral face. 24–25. *Dissomphalus*. 24. External lateral face 25. Internal lateral face. 26–28. Genus B. 26. External lateral face 27. Internal lateral face. 28. Ventral view. 29. Genus D. 29. External lateral face. Dorsal body colored in blue, ventral ramus in red. Scale bar: 100 µm.

Figures 30–38. Male genitalia, lateral view of complex aedeagus. 30. Genus D, internal lateral face. 31–32. *Pristocera*. 31. External lateral face. 32. Internal lateral face. 33–34. *Propristocera*. 33. External lateral face. 34. Internal lateral face. 35-36. *Protisobrachium*. 35. External lateral face. 36. Internal lateral face. 37–38. *Trichiscus*. 37. External lateral face. 38. Internal lateral face. Dorsal body colored in blue, ventral ramus in red. Scale bar: 100 µm.

Figures 39–47. Hypopygium in dorsal view. 39–40. *Calobrachium*. 40. Ventral posterior projection dropshaped. 41. *Pseudisobrachium*. 42. *Zimancus*. 43. *Apenesia*. 44. *Foenobethylus*. 45. Genus B. 46. *Trichiscus*. 47. *Pristocera*. Label: (hp) hypopygeal plate; (shp) subhypopygeal plate. Scale bar: 100 µm, except 39 (50 µm), 40 (20 µm) and 47 (50 µm).

Figures 48–58. Hypopygium in dorsal view, except 48, ventral view. 48. *Pristocera*. 49. *Pristepyris*. 50. *Propristocera*. 51. *Caloapenesia*. 52. Genus A. 53. *Heterocoelia*. 54. *Eupsenella*. 55. *Paraceleroderma*. 56. Genus D. 57. *Protisobrachium*. 58. *Dissomphalus*. Scale bar: 48–50, 200 µm, 51–28, 250 µm.

AGRADECIMENTOS

Os caminhos que me levaram a escrever esta tese começaram a ser percorridos em janeiro de 2000, quando deixei o conforto da casa dos meus pais em Porto Velho-RO para uma jornada que duraria 19 anos em Vitória-ES. Essa jornada não seria possível se eu não tivesse, ao meu lado, pessoas que me apoiaram, me encorajaram e me deram todo o suporte que precisei.

Meus pais são, certamente, os melhores do mundo. Eles permitiram que sua filha caçula fosse morar fora de casa, a quilômetros de distância, e, assim, realizar o sonho de se tornar doutora. Na ocasião, eu achava que me tornaria outro tipo de doutora: médica. Mas acho que esse tipo de doutora serve, não? Pai e mãe, obrigada pela confiança e por todo amor que sempre recebi de vocês.

Irmã querida, obrigada por ser minha grande companheira nessa vida. Seu amor sempre encheu meu coração de esperança e confiaça para continuar lutando pelos meus sonhos. Obrigada pela Gabi e pela Gigi. Minhas eternas nenas.

Irmão, obridada pelo ano e meio mais importante da minha vida. Você me ajudou a colocar em prática todos os ensinamentos dos nossos pais. Ao seu lado, aprendi a ser mais responsável. Jamais me esquecerei do dia que você me ajudou a entender que a Biologia era uma das minhas grandes paixões. Obrigada pelos meus sobrinhos queridos, Heitor e Júlia, que enchem o coração da tia de orgulho.

Agradeço imensamente aos meus tios, Edivanda, Elna, Elias e Erik, que tornaram minha vida em Vitória possível e mais confortável. Tia Edivanda, obrigada por me emprestar seu apartamento, meu lar por três anos. Esse gesto tornou possível minha vinda para Vitória. Tia Elna, obrigada pela generosa doação de todos os seus livros de Biologia. Eles foram e continuam sendo muito úteis e importantes para mim e minha formação. Obrigada, também, pelos conselhos e por me indicar Celso para ser meu orientador. Tio Elias, obrigada por confiar em mim todas as vezes que você aceitou ser fiador dos meus alugueis. Tio Erik, obrigada por sempre me ajudar. Meu primeiro computador foi você quem me deu. Depois dele, pude comprar os outros, sempre com sua ajuda para adquiri-los e consertá-los. Vocês são pessoas incríveis.

Agradeço aos meus avós, Francisco e Carmem, por cuidarem de mim. Não me esquecerei das muitas vezes que chegava em casa e tinha sacolas e sacolas de comidinhas gostosas esperando por mim. Amava passar minhas tardes de domingo escutando as histórias da vovó e depois curtir um sonzinho no DVD com o vovô na sala. Queria poder voltar no tempo para viver isso novamente e escutar a vovó pergutando para mim novamente "Como vão as suas codornas, minha filha?". Minha avó achava que eu trabalhava com codornas (apesar de eu ter explicado para ela que eram vespas).

Gabriel, meu marido, companheiro e pai dos meus filhos. Poucas pessoas podem se igualar a você, um amigo fiel e um companheiro inteligente e imensamente responsável. Tive muita sorte de te encontrar nessa vida. Obrigada por tudo. E obrigada também por sempre revisar meus textos e por traduzi-los para o inglês. Não sei o que seria dessa tese sem o seu apoio.

Agradeço ao meu filho, Miguel, por ter me mostrado o verdadeiro sentido do amor incondicional e por me ensinar a valorizar e aproveitar melhor meu tempo. Em breve, outro pacotinho de amor virá (Murilo

ou Clarice) para tornar minha vida ainda mais completa. Vocês são a minha grande motivação para finalizar essa tese.

Agradeço imensamente a Dona Regina, minha sogra, com querm pude contar para cuidar do Miguel enquanto finalizava esta tese. Sem sua ajuda jamais teria conseguido chegar ao final. Sei que poucas sogras podem fazer o que a senhora fez por mim e, por isso, tenho muita gratidão a você. Obrigada ao meu sogro, Seu Celio, que compreendeu que a ajuda da sua esposa seria muito importante para mim. O senhor fará muita falta.

Agradeço às minhas amigas Fernanda, Lidiana e Juliana. Por muitos anos me acompanharam no laboratório e me ajudaram muito com bons conselhos. Fora de lá elas continuam me acompanhando e sendo muito generosas. Vocês são irmãs que a vida me deu.

Muito obrigada aos amigos Gimu, Edinho, Tamara e Juliano. O apoio e presença de vocês na minha vida me fez sentir como se eu estivesse mais perto de casa. Vocês me fazem sentir querida.

Agradeço muito aos amigos do laboratório. Chirlei e Lucyane, obrigada por serem boas companhias nesses últimos anos de laboratório, pelo carinho e por me ajudarem tanto no dia-a-dia. Agradeço a Geane, Ricardo, Diego, Magno, Cecília, Wesley, Juan e Lim pelos cafés, pelos conselhos, por tirarem dúvidas e por me ensinarem durante todos esses anos. Obrigada, Arturo, por todo ensinamento com o protocolo molecular e com as análises filogenéticas. Obrigada, Bife, pelo convívio e pelas fotos desta tese.

Agradeço ao meu orientador, Celso, com quem convivo há mais de 16 anos. Sua orientação fez de mim uma pessoa melhor. Sou muito feliz por ter conhecido o mundo das vespas parasitoides e por ter tido um orientador competente e apaixonado pelo que faz. Muito obrigada por tudo.

Agradeço aos meus mestres, professores do PPGBan, por todo o conhecimento e conselhos transmitidos. Sempre serão exemplos ao longo da minha vida acadêmica. Agradeço aos membros da banca, que aceitaram ler esta tese e contribuir com minha formação.

Agradeço ao Laboratório de Ultraestrutura Celular Carlos Alberto Redins (LUCCAR/CCS-UFES) pelas imagens de miscroscopia eletrônica de varredura.

Agradeço à CAPES por três anos e meio de bolsa cedidas a mim. E, por fim, agradeço a todos aqueles que de alguma forma contribuíram para minha formação, tanto profissional quanto pessoal.

APRESENTAÇÃO

Entrei na UFES como aluna no inicio de dezembro de 2002. Uma semana depois, iniciei o meu primero estágio voluntário no Laboratório de Sistemática de Bethylidae, sob orientação do professor Celso Azevedo. No início, e por muito tempo, fiz trabalhos muito simples, como trocar álcool das amostras, organizar a coleção líquida de matérial didático, cortar quadradinhos de polipropileno para cobrir fundos das caixas entomológicas, cortar triângulos, fazer etiquetas, montar e etiquetar bichos. Confesso que era um trabalho bem cansativo e um pouco frustrante. Na época, não entendia a importância do que estava sendo ensinado e, sem saber, estava sendo preparada para uma função que pude assumir anos mais tarde na qualidade de técnica bolsista da Coleção Entomológica da UFES. Em agosto do ano seguinte, e antes de assumir um projeto de taxonomia, resolvi sair do laboratório para experimentar outra área. Nesse mesmo mês, iniciei meu segundo estágio voluntário em um laboratório de fisiologia humana (Laboratório de Fisiologia Cardiovascular), sob orientação do professor Helder Mauad, onde eu trabalharia com a ação de plantas ditas como medicinais no controle da pressão arterial: um assunto que me encantou e me fez ansiosa para iniciar meu projeto. Antes disso, ajudei dois colegas do meu laboratório a concluírem seus estudos por um ano e meio. Aprendi muito nesse processo, como, por exemplo, inserir microcateteres em veias e artérias, preparar soluções com volumes micrométricos, fazer extrato hidroalcoólico de *Cecropia peltata* (Embaúba), mexer no espectrofotômetro de chamas, operar em gaiolas metabólicas e, infelizmente, interromper a vida de ratos com injeções letais de HCL. No entanto, o maior ensinamento recebido por mim nesse período foi entender que é necessário aprender a trabalhar coletivamente, a ter paciência e que minha verdadeira paixão eram os insetos. Antes que eu iniciasse meu projeto com *Arnica montana* (Arnica) e sua ação potencialmente tóxica para o sistema cardiovascular, resolvi que estava na hora de voltar para os Bethylidae.

Após meu retorno aos insetos, estava na hora de iniciar meu primeiro estudo na área. Não me sentia preparada para iniciar um trabalho de sistemática de qualquer gênero de Bethylidae (e de fato não poderia estar). Primeiro, sentia que precisava entender o que Bethylidae era, qual seria a identidade de cada gênero ainda desconhecido para mim e a diversidade morfológica da família. Foi quando eu fiz o estudo de perfil de fauna que rendeu o artigo intitulado “Os gêneros de Bethylidae (Hymenoptera: Chrysidoidea) de quatro áreas de Mata Atlântica do Espírito Santo”.

Depois desse estudo, escolhi *Holepyris* como objeto de estudo do meu trabalho de conclusão de curso. Tive muitas dificuldades em determinar os limites entre as espécies desse gênero. Os exemplares apresentavam muitas diferenças corporais e, no entanto, compartilhavam um único padrão de genitália. Desta forma, surgiu a pergunta: o que é determinante para *Holepyris*? O padrão genital ou padrões das demais partes do corpo? Esse estudo não gerou um artigo porque essa pergunta viraria tema do meu mestrado, que iniciaria em 2009.

Durante o mestrado, dei prosseguimento ao estudo dos limites entre as espécies de *Holepyris*. No entanto, precisei abandonar esse projeto por questões operacionais. Eu não sabia como utilizar nem a

cladística nem outros métodos para responder essa pergunta e quais seriam meus critérios para propor o corte – onde cada espécie começa e onde ela termina. Em razão disso, abandonei esse projeto e iniciei outro: *Dissomphalus*, da Tailândia. Durante a execução desse trabalho eu finalmente me encontrei. Apaixonei-me pelo grupo e descobri minha habilidade para o desenho. Esse estudo foi publicado em 2013, sob o título "Revision of Thai *Dissomphalus* Ashmead, 1893 (Hymenoptera, Bethylidae), with description of twenty-four new species", que resultou em uma monografia publicada na revista *Zooataxa*. Durante o mestrado, pude também finalizar o artigo de perfil de fauna do Madagascar (Insecta, Hymenoptera, Bethylidae: range extension and filling gaps in Madagascar), que foi fruto da minha vontade de entender mais sobre a diversiadade de Bethylidae, principalmente dos gêneros de outras regiões zoogeográficas além da região Neotropical (fauna com a qual estava mais habituada). Durante a triagem do material de Madagascar, encontrei alguns exemplares (machos e fêmeas) de *Tuberepyris*, gênero até então monotípico, representado por um único exemplar fêmea. Essa descoberta gerou um artigo intitulado "Three new species of *Tuberepyris* Lanes & Azevedo (Hymenoptera, Bethylidae), with amended diagnosis of the genus".

Sem saber, meu doutorado estava sendo desenhado durante o mestrado. Durante a triagem do material da Tailândia, selecionei exemplares que seriam supostamente *Dissomphalus* sem processo tergal. Após um exame minucioso dos exemplares (fazendo uso de microscopia eletrônica de varredura), percebi que se tratavam, na verdade, de *Protisobrachium* e que esses exemplares tinham edeago complexo, assim como *Dissomphalus*, característica até então dita como exclusiva desse táxon. Após essa descoberta, passei a reinterpretar o padrão de edeago descrito para alguns Pristocerinae cuja descrição citava a presença de valvas. Em 2014, Azevedo publicou a revisão de *Trichiscus*, na qual descreve o edeago complexo presente em todas as espécies do gênero. Sendo assim, haveria muitos outros gêneros com a presença de edeago complexo dentro de Pristocerinae. Diante esses fatos, a definição de *Dissomphalus* precisava ser revisada e o gênero redefinido.

Iniciei meu doutorado com o projeto intitulado "Sistemática Filogenética de *Dissomphalus*" visando a reintepretação do táxon. Selecionei Pristocerinae como grupo interno e iniciei a triagem dos exemplares e, em seguida, a extração de DNA do material. Ao final desse precesso, percebi que, para entender *Dissomphalus*, primeiro seria necessário compreender como o edeago complexo varia dentro da subfamília, bem como entender quais seriam as possíveis hipóteses para a origem desse tipo de edeago. Percebi, também, que eu tinha material suficiente para testar as hipóteses de relacionamentos entre a maior parte dos gêneros de Pristocerinae. Desta forma, eu não apenas levantaria as diferenças morfológicas da genitália de *Dissomphalus*, como também poderia lançar hipóteses para a subfamila como um todo. Sendo assim, o meu projeto passou a ser "Reconstrução filogenética baseada em dados moleculares de Pristocerinae".

Reconstrução filogenética de Pristocerinae (Hymenoptera, Bethylidae) baseada em dados moleculares.

Resumo

Pristocerinae Mocsáry, compostos por 23 gêneros e 1061 espécies, é a subfamília mais especiosa de Bethylidae. O primeiro estudo filogenético feito para compreender as relações entre os gêneros dessa subfamília foi feito por Terayama. Ele que levou em consideração a maioria dos gêneros de Pristocerinae e utilizou caracteres morfológicos para embasar suas hipóteses. Entretanto, Terayama não explorou caracteres presentes no hipopígio e genitália, que são estruturas fundamentais para delimitar os gêneros dessa subfamília. Além disso, Terayama utilizou caracteres diagnósticos dos gêneros como fonte de caracteres para sua matriz e polarizou os caracteres através do uso de um grupo hipotético externo, com estado plesiomórfico para todos os caracteres, que não fornece sinapomorfias robustas para testar o monofiletismo dos gêneros. Sendo assim, este estudo teve como objetivo testar as hipótese de monofiletismo e as relações propostas anteriormente para os gêneros de Pristocerinae, analisando os agrupamentos obtidos a partir dos caracteres morfoestruturais, especialmente os da genitália masculina e hipopígio. A matriz de caracteres foi construída a partir de sequencias dos genes COI, 28S, LW Pol2 e EFa2 de 17 dos 23 gêneros de Pristocerinae. A matriz foi analisada utilizando os métodos de estimativa de máxima verossimilhança e inferência baysiana. Como resultado, todos os gêneros de Pristocerinae foram recuperados como monofilético, exceto *Acrenesia*. *Pseudisobrachium* foi recuperado em um clado separado de todos os outros gêneros da subfamília. *Calobrachium*+*Caloapenesia* sempre aparecem juntos como grupo-irmão. O clado formado por (Genus A+*Foenobethylus*+*Parascleroderma*) foi obtido como grupo-irmão da politomia formada por (*Acrenesia*+*Cleistepyris)* e dos clados (*Dracunesia*+*Apenesia* (*stricto sensu*)) e (*Eleganesia*+*Austranesia*). Foi recuperado um grande clado formado por (Genus D+*Prostisobrachium*+*Trichiscus*+Genus B+*Dissomphalus*), grupo-irmão de (*Pristocera*+*Pristepyris*+*Propristocera*). O estado 'parâmero dividido em dois braços' se revelou ser homoplástico dentro de Bethylidae. Em contrapartida, o estado 'edeago dividido em dois ramos' foi recuperado como sinapomorfico e exclusivo aos Pristocerinae.

Palavras-chave: Vespa parasitóide, taxonomia, morfologia, genitália, hipopígio.

Molecular-based Phylogenetic Reconstruction of Pristocerinae (Hymenoptera, Bethylidae)

Abstract

Pristocerinae Mocsáry, composed by 23 genera and 1061 species, are the most numerous subfamily of Bethylidae. The first phylogenetic study carried out in order to understand the relations among the genera of such subfamily was developed by Terayama. He considered most of the genera of Pristocerinae and used morphological characters in order to base his hypotheses. Nevertheless, Terayama did not exploit characters present in the hypopygium and genitalia, which are fundamental structures to delimit the genera of such subfamily. Besides, Terayama used diagnostic characters of the genera as a source of characters for his matrix and polarized them through the use of a hypothetical external group, with plesiomorphic state for all characters, which does not provide robust synapomorphies to test the monophyletism of the genera. Therefore, this study aimed at testing the hypotheses of monophyletism and the previously proposed relations for the genera of Pristocerinae, analyzing the obtained groupings out of the morphostructural characters, especially those of male genitalia and hypopygium. The matrix of characters was built from the sequences of genes COI, 28S, LW Pol2 and EFa2 for 17 of the 23 genera of Pristocerinae. The matrix was analyzed through the use of the estimation methods of maximum likelihood and bayesian inference. As a result, all genera of Pristocerinae were recovered as monophyletic, except *Acrenesia*. *Pseudisobrachium* was recovered in a clade separated from all other genera of such subfamily. *Calobrachium*+*Caloapenesia* always appear together as sister-group. The clade formed by (Genus A+*Foenobethylus*+*Parascleroderma*) was obtained as sister-group of the polytomy formed by (*Acrenesia*+*Cleistepyris)* and the clades (*Dracunesia*+*Apenesia* (*stricto sensu*)) and (*Eleganesia*+*Austranesia*). A great clade formed by (Genus D+*Prostisobrachium*+*Trichiscus*+Genus B+*Dissomphalus*), sister-group of (*Pristocera*+*Pristepyris*+*Propristocera*) was recovered. The state ‘paramere divided in two arms’ turned out to be homoplastic within Bethylidae. As opposed to that, the state ‘aedeagus divided in two rami’ was recovered as synapomorphic and exclusive to the Pristocerinae. The analyses obtained in this study support the hypotheses of four new genera within the subfamily that were here described and illustrated.

Keywords. Parasitoid wasps, taxonomy, morphology, genitalia, hypopygium.

1. INTRODUCTION

Among the eight subfamilies of Bethylidae, Pristocerinae Mocsáry are the most numberous one: they are composed by 23 genera and 1061 species (see Azevedo *et al.*, 2018). Pristocerinae, as well as the other Bethylidae subfamilies, are parasitoid wasps known by their high sexual dimorphism in which the male are winged, and the females are wingless and have a reduction of a series of corporal structures. The genera of such subfamily are found in all regions of the world. However, some genera are endemic to a specifc zoogeographic region, which is the case of *Afgoiogfa* Argaman, *Pristocera* Klug, *Pristonesia* Alencar & Azevedo, *Prosapenesia* Kieffer and *Trichiscus* Benoît (Afrotropical region); *Anisobrachium* Kieffer and *Epynesia* Alencar & Azevedo (Palaearctic region); *Calobrachium* Gobbi & Azevedo, *Foenobethylus* Kieffer and *Scaphepyris* Kieffer (Oriental region) and *Dracunesia* Alencar & Azevedo (Neotropical region). This subfamily is currently considered a valid and monophyletic grouping in many classification propostions of Bethylidae (Carpenter, 1999; Terayama, 2003; Carr *et al.*, 2010).

For many years, taxonomic studies have relied only on species descriptions. As time went by, such descriptions became robust and reached a new level in which the beginning of the analysis of the male genitalia and hypopygium was intensified by Evans and, later, Azevedo. Ever since, the male genitalia and hypopygium have been considered extremely important not only for the delimitation of the genera but also their species, once they are highly variable within the generic limit (see Evans, 1964; Terayama, 2003; Alencar *et al.*, 2013; Azevedo *et al.*, 2018). The use of hypopygium characters associated to the genital ones may help in the choice of characters in order to stablish more robust phylogenetic hypotheses, thus allowing their use as a more proficuous source of phylogenetic signals. However important, the morphology of such structures had never been comparatively analyzed until now. With the advent of new technologies and the enhancement of phylogenetic analyses, the study of Pristocerinae gained a new approach with the investigations on the higher-level relationships.

Evans (1964) presented a dendrogram with the possible relations among the genera of Pristocerinae that occur in the Americas, but used highly sexual dimorphism as a distinctive characteristic of such subfamily. In that representation, he used only five genera, namely, *Pseudisobrachium* Kieffer, *Dissomphalus* Ashmead, *Acrepyris* Kieffer (former name for *Pristepyris* Kieffer, junior synonym of *Pristocera* back then), *Apenesia* Westwood (*lato sensu*) and *Parascleroderma* Kieffer.

The first phylogeny study of Pristocerinae would only be published years later by Sorg (1988). Sorg used the same genera Evans did, nevertheless he did not make it clear which cladistic parameters he employed in order to compose the analysis.

Terayama (1996) performed the first cladistic analysis carried out with most genera of Pristocerinae (17 out of the 22 valid genera of the subfamily back then), considering the morphological characters. However, as well as Sorg (1988), Terayama (1996) used genera as terminal taxa. In addition to that, he used diagnostic characters of the genera as a source of characters for his matrix, which does not supply robust synapomorphies in order to test the monophyly of the genera. He also polarized the characters through the

use of an external hypothetical group, with plesiomorphic state for all characters, and used, in his matrix, few informative characters, only 27 out of the 49 analyzed characters. What is more, he did not include the study of the genital structures in his phylogenetic investigation, which is highly important for Bethylidae in general terms.

Carr *et al.* (2010) proposed the first cladistic study that uses molecular characters (28S and 16S genes) in order to base their phylogenetic hypothesis of relationship among the subfamilies of Bethylidae. For that reason, this study relies on only five genera of Pristocerinae, namely, *Dissomphalus*, *Foenobethylus*, *Pristocera*, *Pseudisobrachium* and *Trichiscus*.

Even after the publishing of all these studies, the relations among the genera of such subfamily remain uncertain for a diverse number of reasons: some times due to the obscurity of the method used, and some times because of the taxa selection and used characters. Hence, this study will test the hypothesis of monophyly and relationships former proposed using, so far, the greatest number of terminal taxa for Pristocerinae as well as the greatest number of genes as a source of characters, which are highly used in Hymenoptera, yet still underexploited in the classification of Bethylidae. Furthermore, the obtained groupings will be discussed out of the morphostructural characters, especially the ones in the male genitalia and hypopygium, which will allow a comparative analysis between the taxa and stablish homology hypothesis.

2. MATERIALS AND METHODS

MATERIAL SELECTION AND SORTING

The material used in this study was selected out of ethanol samples from many regions of the world and belonging to many museums and collections (Table 1). The specimens were sorted in genera and selected in order to cover the morphological diversity within each genus present in this study. All in all, 147 specimens were selected as terminal. They correspond to 17 out of the 23 genera of Pristocerinae, three unknown genera that also belong to such subfamily as well as four Bethylinae genera, which were selected as out-group, based on the hypothesis that Bethylinae is the most plesiotypical among Bethylidae (Sorg, 1988; Carpenter, 1999; Carr *et al.*, 2010; Ramos & Azevedo, 2019). Due to the highly sexual dimorphism of Pristocerinae, only males were used in order to facilitate the homology propositions among species. The genera *Afgoiogfa*, *Prosapenesia*, *Anisobrachium*, *Epynesia*, *Pristonesia* and *Scaphepyris* were not included in this study either because of the lack of fresh specimens for DNA extraction.

Almost all Pristocerinae used as terminal taxa of molecular analyses by Alencar *et al.* (50 out of the 58 terminals) were included in this study in order to facilitate the comparison of the results obtained by them. The species *Parascleroderma* sp.1 was analyzed again and it actually is *Foenobethylus*, in this study identified as *Foenobethylus* sp2 ISA273.

The material was provided by the following institutions: **AMNH,** *American Museum of Natural History*, New York, USA; **ANIC**, *Australian National Insect Collection*, Canberra, Australia; **CASC**,

California Academy of Sciences, San Francisco, USA; **CNCI**, *Canadian National Collection of Insects*, Ottawa, Canada; **CPDC,** Centro de Pesquisas do Cacau, CEPLAC, Bahia, Brazil; **CZMA**, *Coleção Entomológica do Maranhão*, Caxias, Brazil; **ISAM**, *Iziko South African Museum*, Cape Town, South Africa; **MNHN**, *Muséum National d'Histoire Naturelle*, Paris, France; **MPEG** Museu Paraense Emílio Goeldi, Belém, Brazil; **NMKE**, *National Museum of Kenya*, Nairobi, Kenya; **QSBG**, *Queen Sirikit Botanical Garden*, Chang Mai, Thailand; **QMSB**, *Queensland Museum South Bank*, Brisbane, Australia; **RMNH**, *Rijksmuseum van Natuurlijke Historie*, Leiden, Netherlands; **UFES**, *Universidade Federal do Espírito Santo*, Vitória, Brazil; **UQIC**, *University of Queensland Insect Collection*, Brisbane, Australia; **YNU** Y*eungnam University*, Gyeongsan, South Korea (J.W. Lee).

EXTRACTION, AMPLIFICATION AND DNA SEQUENCING

The DNA of the specimens was extracted out of the muscles of the male and/or the last segments of the metasoma of the specimens fixed in ethanol with the extraction kit NUCLEOSPIN® (Macherey-Nagel), which followed the protocol of Martinelli *et al.* (2017).

The isolated DNA was used in the polymerase chain reaction (PCR) for the amplification of the fragments of the five genes, in which one is mitochondrial and the other four are nuclear. The selected mitochondrial marker was cytochrome oxidase I (COI), which is one of the most used markers for animals as DNA barcode (Hebert *et al.*, 2003). Among the nuclear genes, the hypervariable region D2–D3 of the 28S ribosomal RNA (28S), which has already been used to recover Bethylidae phylogeny (Carr *et al.*, 2010), was selected as well as the long wavelength rhodopsin (LW), the RNA Polimerase II (Pol2) and the elongation factor-1 α F2 (EFa2), which have been succefully used in phylogenetic inferences of Pompilidae (Hymenoptera, Vespoidea) (Pilgrim *et al.*, 2008; Waichert *et al.*, 2014)

The PCR reactions were standardized with 1 µl of extracted DNA, 2.5 µl of buffer 10 ×, 1.25 µl of MgCl2 (50 mM), 0.3 µl of dNTP (10 mM each nucleotide), 0.3 µl primers (10 µM), 0.125 µl (2.5 U) of Platinum Taq DNA Polimerase (Invitrogen®) and completed with ddH_2O for a final volume of 25 µl. The profiles detailing, primers combination and fragments size are found in Table 2.

The success of the amplification was verified in agarose electrophoresis 1% and quantified with the marker Lugwig ladder® (Biotec). The purification of the PCR product was carried out according to the protocol of the kit ExoSAP-it (USB Corporation).

The sequences were generated through Sanger forward sequencing in the company MACROGEN (South Korea). Each obtained fragment was compared by similarity with the sequences of GenBank (http://ncbi.nclm.nih.gov) using Basic Local Alignment Search Tool (BLAST) in order to confirm whether the fragments in fact correspond to the amplified markers instead of contaminant ones.

MATRIX OF MOLECULAR DATA

The sequences of each gene were analyzed and separately aligned with the use of the program MEGA version 6 (Tamura *et al.*, 2013). The protein coding genes, namely, COI and Pol II, were manually aligned and used the respective sequence of amino acids as reference. The other genes were aligned through the online program MAFFT 7 (Katoh, 2013), out of the algorithm L-INS-i. Some sequences of the genes COI and 28S produced in the study of Alencar *et al.* (2018) (accession Nos MG760739–MG760847) and Carr *et al.* (2010) (accession No GU213952) were incorporated to this study and obtained through GenBank (Table 1).

MOLECULAR PHYLOGENETIC ANALYSIS

The phylogenetic relations were individually infered for each marker as well as for a concatenated matrix with the five partitioned markers, which allows for each partition to present an evolutive model in particular (Table 2).

The phylogenetic inference stage was preceded by the verification of the sequences saturation degree through the program DAMBE 5.0.23 (Xia & Xie, 2001) out of graphs of synonymous and non-synonym substitutions. Partitioning COI and POL2 in three groupings according to the position of the nucleotide of the codon was opted due to the the high saturation in the third nucleotide of the codon of COI and a slight tendency in the third nucleotide of the codon POL2.

The evolutive models were estimated through the program PartitionFinder2 (Lanfear *et al.*, 2016) with the use of the search method *greedy* (Lanfear *et al.*, 2012). The concatenated matrix was partitioned in nine blocks, regarding one partition for each of the genes 28S, POL2 and EFa2 and three for each of the genes COI and POL2, according to the position of the nucleotide of the codon. Among all evolutive models of the program, the one that best fits each of the nive partitions selected through the Bayesian Information Criterion (BIC) found in Table 2 was used.

The phylogenetic trees were inferred out of Maximum Likelihood (ML) and Bayesian Inference (BI) analyses. The ML analysis and support test of the bootstrap branches were carried out in the program RaxML (Stamatakis, 2014), under the platform CIPRES (https://www.phylo.org/portal2). In such analysis, the nine partitions were indicated to the program so that it would estimate the best gamma (G) distributions and the proportion of invariable (I) sites for each partition. The evolution model GTR was chosen for all partitions of the concatenated matrix as well as for each individual gene, once it is the only model implemented by the program. The generated trees were viewed and edited in the program Figtree 1.4.2. (http://tree.bio.ed.ac.uk/software/figtree/), in which clades with bootstrap values equal or greater than 50% were kept and statistic supports greater or equal to 70% were considered high.

For the BI analysis, the phylogenetic trees were inferred in the program MrBayes 3.1 (Huelsenbeck & Ronquist, 2001) and used a number of sufficient generations so that each analysis could reach an average standard deviation of the frequencies below 0.01 and the value of the potential scale reduction factor near 1.

Such parameters indicate the convergence of the chains in a stationary distribution. In average, 10 million generations were sufficient to obtain the parameters in the individual analysis of each gene, while 60 million generations were necessary for the concatenated matrix. The phylogenetic trees and respective posterior probabilities were summarized with the use of 25% burn-in. The generated trees were viewed and edited in the program Figtree 1.4.2, in which only clades with posterior probability equal or greater than 95% were considered significant. Clades with posterior probability inferior to 50% were collapsed.

ILLUSTRATIONS

The specimens were photographed with the aid of a Leica Z16 APO stereomicroscope fitted with a camera adaptor coupled to a Leica DFC 295 video camera (LeicaMicrosystems, Germany). The pictures of head, mesosoma and metasoma were produced from stacks of images that vertically transected the specimen using Leica LAS (Leica Application Suite V4.3.0) Microsystems by Leica (Switzerland) Limited. These were automatically combined into a single image using Helicon Focus (version 6.3.6; HeliconSoft, Dominica), based on Method C (Pyramid) and focus autoadjustments 1% (horizontally). A scaleable and modular LED illumination dome for microscopic scientific photography was used, as described by Kawada & Buffington (2016). The hypopygium and male genitalia drawings were performed through the use of a camera lucida attached to an Olympus CH30 light microscope and posteriorly digitalized by an image editor. The micrographs were obtained through the use of a Jeol JSM-661 scanning electron microscope (SEM). In order to obtain SEM images, the structures were either washed in alcohol 100% or acetone 100% (in the case of the *Pseudisobrachium* genitalia) and dried in room temperature. The structures were mounted on stubs using a double-sided carbon tape, then coated with gold (Desk V; Denton Vacuum, Moorestown, NJ, U.S.A.) and finally observed with a scanning electron microscope (JEOL, JEM6610 LV) at Laboratório de Ultraestrutura Celular Carlos Alberto Redins in the Health Science Center (LUCCAR/CCS-UFES). The genitalia used to illustrate the genera that have the complex aedeagus were cut sagitously, splitting the dorsal body in halves and separating the two pieces that compose the ventral ramus.

TERMINOLOGY AND TREATMENT

The terminology for general body structures follows Azevedo *et al.* (2018), Mugrabi & Azevedo (2013), Kawada *et al.* (2015) and Alencar *et al.* (2018). Integument sculpture terminology follows Harris (1979). The measurements that refer to the hypopygium follow Mugrabi & Azevedo (2013).

3. RESULTS

The phylogenetic hypotheses obtained in the ML (Fig. 1) and BI (Fig. 2) analyses were similar and in all of them six great clades were obtained, all of those with the same taxa composition (clade A to F, figs. 1–2). Nevertheless, the relations among two of these great clades were not the same in these different analyses.

For BI, Clades E and F behave as sister-groups, while Clade F, for ML, appears as a sister-group of Clade E+(Clade C+Clade D).

In both analyses, all genera were confirmed as monophyletic, except for *Acrenesia* Alencar & Azevedo, which formed two separated clades with high supports (PP= 100; B=100 for both). In all analyses, *Calobrachium* and *Caloapenesia* Terayama are recovered as sister-groups and *Pseudisobrachium* always forms a clade separated from these taxa and from all the other genera of the subfamily (PP = 100; B =100). Genus A, *Foenobethylus* and *Parascleroderma* form a clade (PP = 93; B = 75), sister-group of the clade constituted by polytomy of *Acrenesia*+*Cleistepyris* Kieffer (PP = 99; B = 41) and of the clades *Dracunesia*+*Apenesia* (PP = 59; B = 31), *Eleganesia* Alencar & Azevedo and *Austranesia* Alencar & Azevedo (PP = 76; B = 28). Genus D+*Prostisobrachium* Benoît+*Trichiscus*+Genus B+*Dissomphalus* formed a clade (PP = 100; B = 98). The relations among these taxa vary according to the carried out analyses. According to BI, *Trichiscus* is a sister-group of Genus B+*Dissomphalus* (PP = 100). However, in ML, the relation is *Dissomphalus* as a sister-group of *Trichiscus*+Genus B (B = 91). Finally, *Pristocera* was recovered as a sister-group of *Pristepyris*+*Propristocera* Kieffer (PP = 100; B = 100).

4. DISCUSSION

Ever since the publishing of Bethylidae by Haliday (1839) until now, the focus and type of generated descriptions have been evolving. Nowadays, the importance of the study of the male genitalia and of hypopygium in Bethylidae is common sense and, due to that, the descriptions and illustrations of such structure have become part of the studies of taxonomy of the species and genera of the family. Especially for Pristocerinae: the male genitalia and hypopygium have an important meaning. That happens because at the same time these structures keep an identity that is attributed to a common descendency sharing (generic characters), they have attributes that are highly variable and that may relate to the species in a clear way. For Pristocerinae, the variations of the format of these structures tend to be more discontinued (see for instance Evans, 1963 and Waichert & Azevedo, 2004) when compared to Epyrinae (see for instance Evans, 1969 and Azevedo, 2011), which facilitates the use of their morphology in the delimitation of the taxa of the subfamily.

In addition to the enhancement of the quality of taxonomy publishings, there has been an increase of studies that have struggled to stablish the phylogenetic relations of Bethylidae as well as the resolution for problems concerning the limits among the genera of such family. Studies like the ones proposed by Terayama (1996), Carr *et al.* (2010), Zamprogno & Azevedo (2014) and Alencar *et al.* (2018) were important in order for the scientific community to advance the understanding of Bethylidae. Those studies have supplied the scientific community with phylogenetic relations and taxonomic decisions that are either sustained in this paper or refuted. Therefore, the definition on the genera and the characters that define them are as follows in this thesis.

ON DOUBLE PARAMERE

Caloapenesia, *Calobrachium* (clade A) and *Pseudisobrachium* (clade B) are genera easily differentiated from the other ones in Pristocerinae because they have male genitalia with paramere composed of two arms articulated to the basiparamere. The discovery of Genus A (Clade C) made it become the fourth genus of the subfamily to present such characteristic (Figs. 65, 68, 78, 81). The character 'double paramere' would seem to be homologous to these taxa. However, as opposed to what was expected, it turned out to be homoplastic. A more precise analysis of the parameres has revealed that more importantly than having 'double paramere' it is how they are displayed in the genitalia.

Some previous studies demonstrated that, though the genera had double paramere, there was an uncertainty about the homology among them. Gobbi & Azevedo (2010), while characterizing *Pseudisobrachium* (Fig. 8), defined that the insertion of the dorsal paramere on the basiparamere is lateral. the position of the articulation of the dorsal paramere is underneath to the apical margin of the basiparamere and that the dorsal paramere is close to the ventral paramere. We concluded that only when observed the high magnifince images of scanning electron microscope (SEM).

Zamprogno & Azevedo (2014) differentiated *Caloapenesia* (Figs. 3–4) from *Pseudisobrachium* by the position of the insertion of the dorsal paramere in the basiparamere, being the latter dorsal in *Caloapenesia*. Later, Gobbi & Azevedo (2016) pointed the similarity among *Calobrachium* (Fig. 6) and *Caloapenesia* as to the relation of the insertion of that structure, which is also dorsal and, like in *Pseudisobrachium*, also articulate with the basiparamere in the subapical portion, and that the dorsal paramere is close to the ventral paramere.

All these morphological differentiations gained strength after the molecular study that recovered the same pattern of characteristics sharing, once clade A does not include *Pseudisobrachium* as its member. Nevertheless, Genus A, which also has dorsal lateral paramere, as well as *Calobrachium* and *Caloapenesia*, did not cluster group as them. Besides that characteristic, there were many others that allowed the supposition that the relation of sister-group would be stablished among them, and not *Foenobethylus* and *Parascleroderma* (Clade C), as obtained. Among these characteristics, one could name: pronotal flange subvertical; hypopygium not divided, forming a single plate, with median ventral surface fully sclerotized and flat, median hypopygeal stalk short (smaller than hypopygium plate lengths) and slender, lateral hypopygeal stalk present and very short (Fig. 52); male genitalia with paramere double, dorsal arm of paramere inserted dorsally into basiparamere, straight and slightly sclerotized (Figs. 65, 68, 78, 81); basiparamere with hyaline basal and dorsal projection covering the base of aedeagus (Figs. 65, 78); basal ring complete and well developed; basivolsella slender and long, touching the genital ring (Figs. 67, 80), without vannus; and aedeagus composed by one ramus. It is known that the set of these characteristics is important for the morphological and taxonomic design and, for being monotype in the tree, the relation of Genus A with the other taxa may not have been well sampled. However, all the characteristics may represent

homoplastic conditions. The inclusion of a higher number of specimens may reinforce the stablishment of sister-group hypothesis for this taxon as well as broaden the understanding of these characters.

OTHER BETHYLIDAE TAXA

Having double paramere is not exclusive of the above taxa, much less Pristocerinae. That characteristic has already been observed in Bethylidae, genera such as *Goniozus* Förster, *Lytopsenella* Kieffer, *Prosierola* Kieffer and *Eupsenella* Westwood (see Ramos & Azevedo, 2012 and 2018), in all genera of Mesitiinae (see Barbosa & Azevedo, 2011, 2012 and 2014), and Scleroderminae, genera such as *Plastanoxus* Kieffer, *Glenosema* Kieffer and *Sclerodermus* Latreille (see Evans, 1978).

The analysis of the genitalia of Bethylinae and Mesitiinae revealed that the patterns of the double paramere are a lot different from the ones found for Pristicerinae. In Bethylinae, the dorsal arm of paramere articulates with the apical margin of the basiparamere and the dorsal and lateral arms of paramere are very close to each other and have similar sizes and shapes (Fig. 11). In Mesitiinae, the articulation is much more underneath than Pristocerinae and, thus, there is a significant distance among the dorsal and lateral arms of paramere. Besides, the shapes of the paramere are quite different when compared with each other, in which the dorsal is always thin and long (Figs. 12–16). As for the pattern seen in Scleroderminae, it is similar to the one found in *Caloapenesia*, *Calobrachium* and Genus A. The dorsal paramere is, in general, long and well sclerotized, articulating with the basiparamere in its median portion and facing the dorsal surface of the genitalia.

According to Carpenter (1999), Bethylinae are considered more basal within Bethylidae. It is based on that fact that presenting ‘double paramere’ is a plesiomorphic condition for the paramere in Bethylidae. Furthermore, since the pattern of the double paramere of Bethylinae is different from the ones of Pristocerinae and Scleroderminae and those of Mesitiinae, it is important to point out that not only the presence of a second paramere but also its articulation in the apical margin of the basiparamere make of it an equally plesiomorphic condition.

Due to that, there are three general patterns of shape and dorsal paramere connection in Bethylidae that reveal some importance in the differentiation of the taxa that have double paremere within the subfamily. Nevertheless, all these genera – which genitalia have two paramere – generally present common characteristics, for instance: genital ring ventrad, genital ring complete and well-developed, basivolsella close to the other, covering aedeagus ventrally, and basiparamere with hyaline, dorsal and basal projection covering the base of aedeagus (Figs. 5, 7, 9, 12, 15, 65, 78). Therefore, these characteristics seem to represent some kind of adaptive convergence to the homoplastic character ‘double paramere’ and, thus, the differentiation of how it is present in the genitalia will help the search for synapomorphies for these groups.

ON APICAL PROJECTION OF BASIPARAMERE

Apenesia, *Austranesia* and *Dracunesia* present a short projection in the apical portion of the basiparamere (Figs. 17, 18; see Alencar *et al.* (2018) figs. 7 D–E, 8 F–G, 9 F–G). Such projection is dorsally located besides each paramere, and is short and apical (ie, dorsal paramere) of *Caloapenesia*, *Calobrachium* and *Pseudisobrachium*. However, as a structure that begins in the basiparamere and has insertion similar to the one found in Bethylinae, it could be mistaken as an additional arm of the paramere. Nevertheless, the SEM micrographies of the genitalia of the four genera showed us that the projection of *Apenesia*, *Austranesia* and *Dracunesia* is different from the projection of all the other genera that effectively have double paramere, once their projection is continuous with the basiparamere, with no sign of articulation between the projection and the basiparamere, differently from the others, which always present basal articulation. Thus, this apical projection and the double paramere cannot be treated as different conditions of the same transformations series.

CLADE B

Pseudisobrachium seems to be a unique genus within Pristocerinae. It never formed a clade with the other genera of Pritocerinae, not even with those that share the character 'double paramere'.

Terayama (1996) proposed the clade ((*Pseudisobrachium*+*Protisobrachuim*)+*Neoapenesa*), the latter currently classified as *Apenesia*, by Alencar *et al.* (2018) based on lacking or indistinct notauli and the hypopygium three stalk. These two characteristics are weak to support such clade.

As for the lacking notauli, though *Apenesia* does not have it in fact, Terayama (1996) came to that conclusion for the other genera regarding the analysis of the specimens that do not represent the general pattern of *Pseudisobrachium*, once many species of such genus have notauli present in all variable states of shape and conspicuity (see Azevedo, 2008; Gobbi & Azevedo, 2010). The notauli of *Protisobrachium* Benoît are also present, though they are short and thin in *P. gracile*.

As for the three hypopygeal stalk, that is a very common characteristic within Bethylidae, including in *Pseudisobrachium* and *Protisobrachuim*. There are one-off cases in which the three stalks are not present, like in *Pristocera*, in which only the median stalk is present (Figs. 47–48), or in *Caloapenesia* (Fig. 51) and *Calobrachium* (Fig. 39), in which the absence or presence of the lateral stalk is considered interspecific variation or even among the genera of Mesitiinae (see Barbosa & Azevedo, 2011; 2012; 2014), which present only one median stalk that can be simple or bifurcated (Figs. 42, 53).

Most of the previous authors of Bethylidae have treated the hypopygium as a simple lamina. However, the samples of all genera have one extra lamina, which lays over the inner surface of the hypopygium. This subhypopygeal plate is membranous, and it is usually collapsed. Nevertheless, sometimes this inner plate can be more sclerotized to such an extent that it can be easily confused with the main hypopygeal plate. *Apenesia* represents a striking case within Bethylidae regarding this aspect of hypopygium. Alencar *et al.* (2018) stated that *Apenesia* has long median hypopygeal stalk, ie, when the stalk

is longer or equal to half of the total length of the hypopygium. Actually, the best way to characterize it is as absent or inconspicuous. As a matter of fact, there is one rectilinear structure projected in the position where the median hypopygeal stalk would be, but such projection would only be the membrane over the inner surface of the hypopygium, the subhypopygeal plate (Fig. 43). Thus, this median stalk is indeed a part of subhypopygeal plate rather than hypopygeal plate. There is a possibility for such subhypopygeal plate to play the role of the median stalk, but it would be necessary to closely investigate the muscles associated with the plate in order to avoid wrong interpretations of such character and not make wrong comparisons and, thus, wrong primary homology hypothesis. In other words, they would not belong to the same transformations series.

As for the relation among *Pseudisobrachium* and *Protisobrachuim* recovered by Terayama (1996), it was sustained by the setation of the eyes and by the metapectal-propodeal complex longer than wider. In fact, *Protisobrachium* displays characters that are ver similar to *Pseudisobrachium*, probably due to the convergence caused by the general elongation of the body. But the setose eyes and metapectal-propodeal complex are present in many other genera of Pristocerinae, including Genus A and *Caloapenesia*, for instance.

Carr *et al.* (2010), in their concatenated analysis of 16S and 28S, recovered *Pseudisobrachium* as sister-group of *Pristocera* (PP=100 and B=87). Such result was obtained from the reduced number of taxa in the analysis, which used only these two taxa in order to make that hypothesis.

The cladograms obtained by Zamprogno & Azevedo (2014) with the use of morphological data and parcimony analysis and the ones obtained by Alencar *et al.* (2018) through Bayesian analysis with the use of the genes COI and 28S rDNA corroborate the data of this study for *Pseudisobrachium*, once it did not form group with *Caloapenesia* nor any other genus of Pristocerinae involved in the study. The results may indicate that *Pseudisobrachium* can be, in fact, a unique taxon within Pristocerinae, which also reunites unique characteristics such as dorsal paramere inserted laterally, presence of vannus in the basivolsella (Figs. 8, 10) and hypopygium entirely fused to subhypopygeal plate, which is entirely well sclerotized and, generally, ornate.

CLADE C

The morphological explanation that would justify the relation of Genus A with *Foenobethylus* and *Parascleroderma* is unknown. The relationship between *Foenobethylus* and *Parascleroderma* is so well stablished that it is possible to list many characteristics that support the clade. Some of them are as follows: prepectus wide; forewing with R1 absent and junction of Rs&M and cu-a not angled; hind wing with Sc+R short, jugal lobe reduced; median and lateral hypopygeal stalks long (Figs. 44–55); subhypopygeal plate extends far beyond hypopygeal plate (Fig. 44); male genitalia with paramere simple and apex fully directed mesad (Fig. 20); basivolsella wide and short, not touching genital ring (Fig. 21); aedeagus simple with well marked lateral and apical lobes, separating the lateral aera from the central aera of the aedeagus (Figs. 19–

20). If the position of Genus A is considered correct among Clade C, all those characteristics would become meaningless or should be considered a reversion for Genus A. As previously stated, such taxon could be poorly positioned due to a sampling problem. Therefore, it is more sensible that Genus A occupies a clade alone, just like *Pseudisobrachium*, here called Clade C'.

The relationship of *Foenobethylus* and *Parasclerodema* (Clade C) was already expected based on the shared morphostructural characters, as recovered in Alencar *et al.* (2018) in the Bayesian analysis based on 28S and COI (PP=100). There is a second genus that is pointed as being related to *Parasclerodema*: *Afgoiogfa*, which was not included in the analysis of this study for the difficulty in obtaining fresh specimens for the extraction. Terayama (1996) recovered the clade *Parasclerodema+Afgoiogfa* based on the following synapomorphies – anterior border of clypeus strongly produced and trapezoidal, ocellar triangle flat and situated well near occipital border and epicnemium of mesonotum absent. If *Afgoiogfa* were in these analysis it would certainly compose Clade C due to the sharing of the characteristics previously cited and some others, like the ones as follows: malar space being reduced; occipital carina complete; prosternum elongated into a neck as long as wide; mesonotum with notaulus; propodeal declivity without median carina; forewing without R1, Rs&M vein oblique and far from stigma 2 × its length; hypopygium with three anterior stalks and the aedeagus stout and cylindrical, as discussed by Azevedo & Lanes (2007). Actually, the best description for the hypopygium and male genitalia, which best defines the three clades, would be: hypopygium with three anterior stalks very long and narrow; aedeagus gibbous and a pair of lateral apical lobes well marked, separating the lateral area from the central portion of the aedeagus; paramere very long with apex fully directed mesad; and basivolsella wide and short, not touching the genital ring.

Azevedo & Lanes (2007) suggested that *Parasclerodema* may not represent a unique genus since the synonymization of *Ceratepyris* under *Parasclerodema* would be controversial. In the proposition of junior synonym, Argaman (1988) justified that *Ceratepyris* must be representative of the female gender of *Parasclerodema*, once *Ceratepyris* is formed only by females and *Parasclerodema* only by males. The justification is arbitrary, but the analysis of this study recovered the monophyly of *Parasclerodema* in which, though the morphological differences were observed as the dorsal pronotal area format, for instance, the patterns of the other structures, including the genital ones, is the same.

CLADE D

A review of *Apenesia* (*lato sensu*), which divided the genus into nine genera based on the analysis of the genes 28S and COI, was recently published by Alencar *et al.* (2018). The analysis of this present study tested seven genera out of the nine mentioned. *Cleistepyris, Dracunesia, Apenesia, Eleganesia, Austranesia* (Clade D) and *Propristocera* (Clade F) had monophyly confirmed and only *Acrenesia*, differently from the other ones, reveled to be paraphyletic. Another difference is that except for *Propristocera*, all the aforementioned genera, which formed one single clade with *Pristepyris* and *Pristocera*. In our analyses,

Apenesia (*lato sensu*) is monophyletic, except for *Propristocera* and the *dissomphaloides* species-group, this latter now allocated in *Dissomphalus*. However, it is a fact that each lineage of Clade D has their own identities and patterns that are very distinct from each other, which was enough to split the old genus *Apenesia* into several genera (Alencar *et al.* 2018).

In this study, *Acrenesia+Cleistepyris* had high support in the BI analysis (PP=99), but low in the ML (B=41). Alencar *et al.* (2018) defend the monophyletism of *Acrenesia* (represented as Lineage F) based on Bayesian and parcimony analyses with implied weighting. Such clade formed two groupings, which were also obtained here. Nevertheless, the relation was not one of monophyly, as it was found by Alencar *et al.* (2018). They characterized the species of the clade F (*Acrenesia*) as representing the largest body-sized Neotropical species of Pristocerinae. However, such clade reunites two groupings with morphological characteristics that are so antagonistic with each other that it is understandable that *Acrenesia* represents a paraphyletic group. The clade formed by *Acrenesia* sp1 DFM158, *Acrenesia* sp12 ISA291 (*Apenesia* sp12), *Acrenesia* sp10 ISA12 (*Apenesia* sp10), and *Acrenesia* sp2 ISA213 (*Apenesia* sp11) in Alencar *et al.* (2018) – from now on called *Acrenesia* large-bodied style – are, in fact, represented by species with the largest body size. Nevertheless, *Acrenesia* sp4 ISA300 (*Apenesia* sp15), *Acrenesia* sp3 ISA298 (*Apenesia* sp13) and *Acrenesia* sp14 ISA299 (*Apenesia* sp14) in Alencar *et al.* (2018) – from now on called *Acrenesia* small-bodied style – have small bodies, about 2.5 × smaller than those of the previous clade. Besides, it is possible to point many characteristics that differentiate *Acrenesia* large-bodied style from *Acrenesia* small-bodied style, as listed in Table 3, which corroborates our hypothesis. The synapomorphy listed by Alencar *et al.* (2018) contemplate a part of the examined specimens, those of the grouping *Acrenesia* large-bodied style. They said that they proposed the genus *Acrenesia* composed of species in the *columbana* and *pilicornis* species group of the genus *Apenesia* (*lato sensu*), but actually the genus was composed by 10 species of the *pilicornis* group *(Ac. angusticeps* (Evans), *Ac. coarctata* (Kieffer), *Ac. elongata* (Evans), *Ac. fusilis* (Corrêa & Azevedo), *Ac. guatemalensis* (Evans), *Ac. ornata* (Evans), *Ac. pilicornis* (Evans), *Ac. punctata* (Cameron), *Ac. reducta* (Evans) and *Ac. tenebrosa* (Evans)), three species of the *exilis* group *(Ac. exilis* (Evans), *Ac. luteola* (Evans) and *Ac. martini* (Evans)) and one species of the *brasiliensis* group *Ac. venezuelana* (Evans). Due to these facts, the scission of *Acrenesia* is necessary in order to attend both the monophyly requisites and the morphostructural groupings presented by *Acrenesia* large and small-bodied styles (see detail at Taxonomic accounts section).

What is more, the monophyly of *Acrenesia* found in the parcimony analysis with implied weighting by Alencar *et al.* (2018) cannot be considered conclusive, once they analyzed only four species of a same species group, *pilicornis* group, *(Ac. angusticeps*, *Ac. fusilis*, *Ac. tenebrosa* and *Ac. elongata*), which represent only the morphological pattern of large-bodied style.

Here, *Cleistepyris* stablished relationship with *Acrenesia* large and small-bodied styles, differently from what was found by Alencar *et al.* (2018), in which the relation found was the one with *Apenesia* and *Paraseclerodermа+Foenobethylus*. In fact, there are morphological characters that can be comparable

among *Cleistepyris* and *Parasecleroderma+Foenobethylus*, such as the following, for example: the general format of the aedeagus, with well marked lateral and apical lobes, separating the lateral aera from the central aera of the dorsal body (Figs. 19–20; and fig. 8L in Alencar *et al.* 2018), basivolsella short and wide (Fig. 21; and fig. 8K in Alencar *et al.* 2018) and format of anterior margin of hypopygium, with lateral stalk close to the anterior corner strongly projected and elongated, also present in *Acrenesia* small-bodied style (Figs. 44, 55, 105, 114; and fig. 8J in Alencar *et al.* 2018). However, there are more shared similarities among *Acrenesia* long+small-bodied styles and *Cleistepyris* than the taxa involved in the relationship proposed by Alencar *et al.* (2018). The general format of the aedeagus and basivolsella mentioned above are characteristic in many more groups, once it is present in all taxa of clade G (Clade C+D, except Genus A) and Clade F. In a differentiated way, *Parascleroderma* and *Foenobethylus* have aedeagus globoid and paramere laminar (Figs. 19–20), while the taxa of Clade D have aedeagus more elongated and tubular paramere. The clade *Acrenesia* long+small-bodied styles and *Cleistepyris* share characteristics that corroborate the relation of sister-group here proposed as the following: ventral side of occipital carina strong; propleuron not visible in dorsal view, lateral of prosternum not visible in ventral view; forewing with R1 long; hind wing with Sc+R short; genitalia with basiparamere dorsally very narrow, almost absent, paramere tubular with apex gibbous, with apex very wide, base narrow and with escavation to accommodate cuspis.

The relation of sister-group between *Dracunesia* and *Apenesia* has low supports (PP=59, B=31). However, it is possible to stablish a similar morphological pattern among these taxa. *Apenesia* is known by the dorsal projection of the basiparamere, as already discussed in ‘double paramere’, defined by Alencar *et al.* (2018) as apical projection on basiparamere with membranous area with chitinous projections (Figs. 17–18). This projection is also present in *Dracunesia* and *Austranesia*, though it is, in general, smaller than the one found in *Apenesia*. Another resemblance that calls attention is the presence of a lamellar and circular margin in the apex of the aedeagus that is projected ventrally and with lateral hypopygeal stalk far from the anterior corner.

Austranesia was recovered forming a clade with *Eleganesia*, though with equally low supports (PP=76, B=28). Just like among the sister-groups previously mentioned, there are similarities among the patterns of the hypopygia and genitalia between *Dracunesia* and *Eleganesia*. Out of all taxa of Clade D, these are the ones that have greater hypopygeal median stalk, at least 1.8 × larger than the hypopygium plate. These two taxa present very long and narrow parameres; basiparamere apical margin without distinction to paramere; digitus disproportionate small to the size of the genitalia; basal ring board and incomplete, present only in the lateral of the genitalia.

The divergence among the values of support and topologies indicates that the relationships among the genera of Clade D are uncertain and deserve a wider investigation. However, what is correct is the fact inside *Apenesia* (*lato sensu*) there are many distinct patterns that represent, in fact, monophyletic groups with high statistical supports.

CLADE H AND AEDEAGUS DIVIDED INTO TWO RAMI (COMPLEX AEDEAGUS)

The relation among Clades E and F were presented in a divergent way between BI and ML. In BI, these clades formed a large monophyletic group (Clade H), though the value of posterior probability was 68. Such clade was not recovered with the same configuration in ML due to the inclusion of Clade C and the value of B for that hypothesis is much less than the one of BI (B = 30). The relation between the taxa of clades E and F seems to make more sense in light of the Bayesian analysis, because all taxa in these clades present an additional piece coupled to the aedeagus and, according to the Bayesian analysis, the origin of such piece would have been unique.

On the course of the history of Bethylidae Taxonomy, there has been two distinct ways of naming the structures of complex-type aedeagus. The first reference to the division of the aedeagus was done for the genus *Dissomphalus* by Evans (1955 [1954]), who described the aedeagus as an exceedingly complex structure, divided into two parts, the most ventral structure called by him ventral rami, arise at the extreme base and extend for most of the length of the aedeagus and what the author called 'main part' or 'dorsal body', which would be the portion of the aedeagus directly connected to the apodeme.

Later, Evans (1958) compared the genitalia of *Propristocera* as being a lot similar to the one of *Dissomphalus* due to the complexity of the aedeagus without knowing that, actually, he was using, as basis, a species that currently is classified as *Dissomphalus* (*Propristocera tridentata* Evans, nowadays with valid name *Dissomphalus denticulatus*, see Alencar *et al.* 2018). Though this comparasion, Evans was correct at noticing the complexity of the aedeagus and, later, Alencar *et al.* (2018) confirmed the presence of that character for *Propristocera*.

Years later, Evans (1964) described the variation of the genitalia in Bethylidae and explained that the aedeagus may be simple or complex and, when it is complex it is convenient to distinguish between ventral, middle, and dorsal lobes, valves, or rami. For Evans, the name rami would then begin to correspond to the narrowest structures connected to the aedeagus, laminar, as the ones found in *Dissomphalus*, for example, and the name valves would correspond to the most robust structures, as the ones found in the aedeagus of *Pristocera* and *Pristepyris*. Out of that definition, all the descriptions that came then adopted such nomenclature, nominally differentiating the parts that compose the aedeagus within Bethylidae. Zamprogno & Azevedo (2014) coded the 'division of the aedeagus' into simple, divided between two or three valves and, at coding it for *Dissomphalus*, considered the genitalia of such taxon as simple, which demonstrates that they, like Evans, did not believe that the rami (dorsal body and ventral ramus) were not comparable to the valves of *Pristocera* and *Pristepyris*.

A fifth genus with complex aedeagus is *Trichiscus*. Though Benoît (1956, 1986) had studied the genitalia of *Trichiscus* and pointed the similarities between such genus and *Dissomphalus*, he did not report the division of the aedeagus in two pieces. The first description of these pieces was carried out by Azevedo

(2014), who described them as aedeagus divided into dorsal body and ventral ramus, just like in the descriptions of *Dissomphalus* as previously made by Evans (*op. cit.*)

Here we demonstrated that, even though neither Benoît (1957) nor Terayama (1995) had described the genitalia of *Protisobrachium*, this is the sixth genus that has complex aedeagus. In general, all the parts of the genitalia of *Protisobrachium* are difficult to be viewed, once they may be translucid, which makes the use of high-resolution microscopes necessary. Finally, we also discovered two other new genera (Genus B and Genus C) with such division.

The analyses of BI and ML indicate divergent hypotheses as for the origin of the complex aedeagus. According to BI, the origin of the additional piece of the complex aedeagus would only be unique and, thus, synapomorphic (Fig. 2). On the other hand, the analysis of ML indicate that such structure would not be synapomorphic. Among such hypotheses, there are two possibilities for the origin of such piece: either it could have arisen once in clade J followed up by a reversion in clade G, then it would be symplesiomorphic; or it may have arisen independently in clades F and E (Fig. 1) then it would be homoplastic. Nevertheless, when the aedeagus of Bethylidae are examined comparatively, the hypothesis of unique origin for the additional piece in a complex aedeagus presented by the BI seems to make sense. The valves of Pristepyris and Pristocera, as defined by Evans (1964) and defined and illustrated by Zamprogno and Azevedo (2014), are interpretations of what does not to make a lot of sense. The dorsal and median valves are actually part of a unique structure (Figs. 1–2 in Zamprogno and Azevedo (2014)). They are the lateral and posterior faces of what Evans (1958) called dorsal body of the aedeagus just like in *Dissomphalus*, once they are part of a unique structure closely connected to the apodeme. The dorsal valve would then be an additional piece to the aedeagus and, comparatively, it would be the ventral ramus described for *Dissomphalus*. Due to that, the term valves is now obsolete, and the nomenclature proposed by Evans (1958) is adopted for all taxa that have such character. In other words, valves and rami are the same structures, so that they should treated as belonging to the same transfomation series in future morphology-based phylogenetic reconstructions.

ON THE MORPHOLOGY OF COMPLEX AEDEAGUS

Here we realized that ventral rami (VR) and dorsal body (DB) follow the same pattern: the basis of the VR is attached to the genital ring; the external lateral face of each pair of VR is connected to the lateral of DB through a membrane (Figs. 26, 28, 35, 37). However, among the genera there are differences of the volume of VR, size and volume of the lateral membrane that is attached to VR and DB and where the internal lateral face of VR is attached to DB.

In *Pristocera* (Figs. 31–32), *Pristepyris* (Figs. 22–23), *Propristocera* (Figs. 33–34) (Clade F), *Protisobrachium* (Figs. 35–36) and Genus D (Figs. 29–30) (part of Clade E), the apex of VR tends not to go over the length of DB. Therefore, the internal lateral face of the apex of VR is closely attached to the basis of the apical lobe of DB (Figs. 32, 23, 34, 36, 30, respectively). The taxa of clade F (except *Propristocera*)

and *Protisobrachium* tend to present more gibbous VR and, probably due to that, a more voluminous membrane that is externally attached to DB.

As for the taxa of clade E, it is possible to separate them into three patterns. The first pattern is viewed in *Protisobrachium* and Genus D, which is more similar to the pattern of clade F, as previously stated. The second pattern is found in *Dissomphalus*, in which the VR has quite variable length and the connection between the internal lateral face of VR (Fig. 24) and DB never begins in its apex (Fig. 25). Such connection can be stablished in the basis of VR or, at its maximum, in the median region of VR (Fig. 25). Thus, a large portion of VR remains free. The third and last pattern is observed between *Trichiscus* and Genus B. In these two taxa, VR is also attached to the apex of DB, but not in its basis, like in the other genera (Figs. 37, 26–27, respectively). Such connection is seen in every extension of the apices. In such case, VR extends internally to the DB, between the apical lobes in the internal face (Figs. 38, 28, respectively), and is only visible when the genitalia are transversally sected in halves and the observation is carried out from the internal face. Therefore, when the genitalia are observed during a lab routine examination, with no sections nor high-resolution microscopes, only part of VR is visible, and it is difficult to distinguish VR from DB (Figs. 37, 26–27). As an example, Azevedo (2014) did not realized that while illustrating only part of what the VR of the studied species of *Trichiscus* in ventral view would be. Nevertheless, the non-illustrated parts of such structure can be viewed in the lateral and dorsal views, revealing how hard it is to understand the limits of the structures in this taxon.

CLADE E

The taxa of such clade share some outstanding characteristics, such as complex aedeagus, clypeus with lateral region very projected and dorsal pronotal area short.

Genus D has complex aedeagus (Figs. 122, 124), but does not present neither clypeus with lateral region very projected (Fig. 116) nor dorsal pronotal area short (Fig. 118), as the taxa of Clade E. The species of such taxa have characteristics that are similar to *Acrenesia* large-bodied style, *Apenesia*, *Austranesia*, *Cleistepyris* and *Dracunesia* (Clade D), such as dorsal pronotal area as long as anteromesoscutum or nearly so; anteromesoscutum with parapsidal signum and notaulus complete anteriorly or nearly so (Fig. 118); median hypopygeal stalk long; lateral hypopygeal stalk near the anterior corner of hypopygium (Fig. 123); and subhypopygeal plate extending far beyond the hypopygeal plate, these two latter are also found in *Protisobrachium* (Fig. 57). Despite the differences, there are similarities between Genus D and its sister-group *Protisobrachium*, such as: body and antenna elongated, apical lobe of dorsal body very gibbous and ventrad; and basal ring present. *Protisobrachium* and Genus D are the only ones of such clade that basal ring is present, though the ring of *Protisobrachium* is entirely dorsally located and in Genus D it is latero-dorsal.

The monophyletism of *Dissomphalus* as well as its sister-group relation with *Trichiscus* has already been demonstrated by Terayama (1996) in his morphology-based phylogeny and by Carr *et al.* (2010) in their molecular-based study. Here, a broader sampling and new genes were used, which reinforced such

statement (Figs. 1–2). The similarity between these taxa has already been noticed in *Trichiscus* by Benoît (1956), who, in the original description, said *Trichiscus* would be "identical to *Dissomphalus*", except for having "third metasomal tergum narrower than the other ones" and "trichome situated in the third tergum." Currently, we point other similarities, such as aedeagus divided into two rami (Figs. 37–38), as described by Azevedo (2014), and translucid and hypertrophied ramus from digitus, as demonstrated by Mugrabi & Azevedo (2016), characteristic already pointed out by Benoît (1986) as being exclusive of *Trichiscus.*

In spite of that, specimens not identified as being either *Dissomphalus* or *Trichiscus* were analyzed and, hence, treated as Genus B. In the inclusion of Genus B, *Dissomphalus* is, then, sister-group of the clade formed by *Trichiscus*+Genus B (Figs. 1–2). The individuals of such group, Genus B, have the same characteristics shared with the other two genera, like the general aspect of the head (Fig. 84) and mesosoma (Fig. 86), presence of tergal process (Fig. 88) and divided aedeagus (Figs. 26–27, 89–90, 92). Despite such similarities, there are characteristics that distinguish Genus B from *Dissomphalus* and *Trichiscus* and that corroborate with the hypothesis that Genus B represents a new genus, different from *Trichiscus*, such as: difference in the shape and inconspicuity of median carina of clypeus that are similar to the ones found in the taxa of Clade D; tergal process entirely located in the third metasomal tergum (Fig. 88) (though there are some that do not present tergal process). In *Dissomphalus*, whose tergal process is situated in the second tergum, there are species without tergal process and such condition was described by Azevedo (2003) as a secondary loss of structure. For *Trichiscus*, the tergal process is located between the second and third metasomal terga, though there are those without such structure; as for the hypopygium, Genus B has a shape that is similar to the pattern viewed in *Trichiscus* (Figs. 46, 45, respectively), with posterior margin deeply emarginate. However, differently of *Trichiscus*, the specimens presented thickening and high degree of sclerotization of the margins of the subhypopygeal plate.

The relation of sister-group among *Dissomphalus*, *Trichiscus* and Genus B (Clade I) remains uncertain. Relation among the genera apart, the taxa of clade I share unique characteristics within Pristocerinae, such as: body tending to be robust, though short, and presence of tergal process between second and third metasomal segment, even though with reversions, these are the only ones to present such character. The values of support of rami and posterior probability are equally high and, due to such criterion, it is difficult to know which hypothesis would be more robust regarding the relationship among these taxa. Nevertheless, the hypothesis of ML brings a history of relationship concerning to morphological data (Fig. 1). According to such hypothesis, *Dissomphalus* would be the sister-group of *Trichiscus*+Genus B. When present, the tergal process of *Dissomphalus* is always located on metasomal tergum II, while in *Trichiscus* and Genus B it is located on tergum III with a shortening of metasomal tergum II. The difference between these two latter genera is that in *Trichiscus* the tergal process tends to be more lateral and closer to the posterior margin of tergum II and in Genus B it is located more dorsally and in the middle of tergum III. A second characteristic that unites *Trichiscus* and Genus B is the connection between RV in the apex of DB, as

discussed in the topic ‘On the Morphology of Complex Aedeagus’, which is distinct from the one observed in *Dissomphalus*.

CLADE F

The lineage recovered here composed by *Pristepyris*, *Pristocera*, and *Propristocera* was already found by Alencar *et al.* (2018), and among *Pristocera* and *Propristocera* by Zamprogno & Azevedo (2014). These taxa are very similar one to another. They share for instance complex aedeagus (Figs. 22–23, 31–32, 33–34, respectively), and large body size, measuring up to 25 mm, as in *Pristocera* (see Zamprogno & Azevedo (2014)). The relation between *Pristocera* and *Pristepyris*, for example, was already discussed by Evans (1963), when demoted *Pristepyris* to the status of subgenus of *Pristocera* and, later, by Terayama (1996) who undid such synonymy.

In such clade, a unique modification of the hypopygium within the family is present, as described by Zamprogno & Azevedo (2014). In *Pristocera*, there is a deep excavation of the posterior margin that extends until the internal portion of the median hypopygeal stalk (Figs. 47–48). In *Propristocera*, the hypopygium has a inner surface that is little sclerotized (Fig. 50). However, in *Pristepyris* there is not any modification in such structure (Fig. 49), which might indicate a possible case of reversion of this condition.

Pristocera always appears as sister-group of *Pristepyris* in our analyses. The fact that *Pristocera* is the only taxon with deep excavation of the hypopygium makes it, in fact, distinct from all others. Besides, its hypopygium does not have lateral stalk, as in *Calobrachium* and *Caloapenesia*, even though the absence of lateral hypopygeal stalk in the two latter genera is not a rule like in *Pristocera*. Zamprogno & Azevedo (2014) coded the length of the median hypopygeal stalk as short in *Pristocera*, restricted to the very short anterior area not divided. However, there are muscles inserted along the projected anterior area of the plate, which lead us to believe that this whole area is the median stalk, independently if it is divided or not internally, as in all other groups of Bethylidae. .

Pristepyris and *Propristocera* share more characteristics among each other than *Pristocera*, such as: pterostigma very enlarged, much larger than in *Pristocera*; junction of Rs&M and cu-a not angled, median hypopygeal stalk narrow (Figs. 49, 50, respectively), lateral hypopygeal stalk present, subhypopygeal plate fully weakly sclerotized, genitalia with basal ring, and aedeagus with ventral ramus with free apical region, not attached to the dorsal body by membrane (Figs. 22–23, 33–34, respectively), whereas in *Pristocera* the junction of Rs&M and cu-a is angled; the median hypopygeal stalk is wide (Figs. 47–48), the lateral hypopygeal stalk is absent; the subhypopygeal plate is mostly sclerotized; the genitalia without basal ring, and the aedeagus without any free pieces (Figs. 31–32). These morphological similarities between *Pristepyris* and *Propristocera*, and dissimilarities between them and *Pristocera* corroborate our results regarding the relationship among these genera.

5. FINAL REMARKS

The recent studies focusing on Pristocerinae allowed us to better delimited alpha taxonomically and outlined phylogenetically their genera. However, there still are issues to be addressed, such as, the relations between the taxa of Clade E and Clade F among the other genera of Pristocerinae; the sister-group relation among *Dissomphalus*, *Trichiscus* and Genus B; and the positioning of Genus D and Genus A as well as the hypothesis for the possible reversion of the character complex aedeagus for Genus D and for the homoplasy of the character double aedeagus for Genus A, *Pseudisobrachium*, *Caloapenesia* and *Calobrachium*. The inclusion of new specimens for the genera in monotypy in this study as well as the adding of new genes and the inclusion of an analysis based on morphostructural characters would certainly enrich the understanding of such subfamily.

We highlighted the role played by the genitalia and hypopygium in our taxonomic decisions. Nowadays, it is impossible to carry out a good taxonomic study in Pristocerinae without the analysis of these structures. Nevertheless, the genitalia and hypopygium are very variable. Thus, it is hard sometimes to to formulate primary homology hypotheses. One way to stablish safer hypotheses would be to make them out of compared morphology studies with associated musculature analysis. That will allow an advance not only in the studies of Pristocerinae but also Bethylidae. From that point of view, it will be possible to test hypothesis like the ones proposed here, such as the absence of median hypopygeal stalk in *Apenesia* or those regarding the homology of complex aedeagus in the many genera of Pristocerinae, for example. Thus, it will be possible to advance into better understanding the fauna of world Bethylidae.

Finally, we would like to emphasize the necessity of the study of morphology based on scanning electronic micrographies, because such images deepen our capacity of how to interpret the structures like genitalia or other small structures, for instance the tarsal claws and microtexture of integument as demonstrated by Antunes-Carvalho *et al*. (2019) for the beetles Cholevinae.

6. REFERENCES

Alencar, I.D.C.C., Azevedo, C.O., 2013. Reclassification of Epyrini (Hymenoptera: Bethylidae): a tribal approach with commentary on their genera. Syst. Entomol. 38, 45–80.

Alencar, I.D.C.C., Waichert, C., Azevedo, C.O., 2018. Opening Pandora's box of Pristocerinae: molecular and morphological phylogenies of *Apenesia* (Hymenoptera, Bethylidae) reveal several hidden genera. Syst. Entomol. 43, 481–509.

Antunes-Carvalho, C., Ribera, I., Beutel, R.G., Gnaspini, P., 2019. Morphology-based phylogenetic reconstruction of Cholevinae (Coleoptera: Leiodidae): a new view on higher-level relationships. Cladistics 35, 1–41.

Azevedo, C.O., 2003. Synopsis of the Neotropical *Dissomphalus* (Hymenoptera, Bethylidae). Zootaxa. 338, 1–74.

Azevedo, C.O., 2008. Characterization of the types of the Neotropical *Pseudisobrachium* (Hymenoptera, Bethylidae), with a key to species. Rev. Bras. Zool. 25, 737–801.

Azevedo, C.O., 2011. Synopsis of *Aspidepyris* Evans, 1964 (Hymenoptera, Bethylidae). Zootaxa. 3016, 63–68.

Azevedo, C.O., 2014. Revision of *Trichiscus* Benoît, 1956 (Hymenoptera, Bethylidae). Zootaxa. 3802, 318–334.

Azevedo, C.O., Alencar, I.D.C.C., Ramos, M.S., Barbosa, D.N., Colombo, W.D., Vargas, J.M.R., Lim, J., 2018. Global guide of the flat wasps (Hymenoptera, Bethylidae). Zootaxa, 4489, 1–294.

Azevedo, C.O., Lanes, G.O., 2007. Rediscovery of the Oriental *Foenobethylus gracilis* with discussion of allied genus. Mitt. Int. Entomol. Ver. 32, 133–141.

Barbosa, D.N., Azevedo, C.O., 2011. Order Hymenoptera, family Bethylidae, subfamily Mesitiinae. In: van Harten, A. (Ed.), Arthropod Fauna of UAE. Vol. 4. Dar Al Ummah Printing, Publishing, Distribution & Advertising, Abu Dhabi, pp. 375–404.

Barbosa, D.N., Azevedo, C.O., 2012. Revision of Mesitiinae (Hymenoptera, Bethylidae) from Madagascar, with description of eleven species. Zootaxa 3417, 1–44.

Barbosa, D.N., Azevedo, C.O., 2014. *Moczariella*, a bizarre new genus of Mesitiinae (Hymenoptera, Bethylidae) from Arab Peninsula. Zootaxa 3860, 291–297. 7

Benoît, P.L.G., 1956 Contributions à l'étude de la faune entomologique du Ruanda-Urundi (Mission P. Basilewsky 1953). Hymenoptera: CXII. Bethylidae. Ann. Mus. R. Congo Belge. Sci. Geol. 51, 560–564.

Benoît, P.L.G., 1957. Hymenoptera—Bethylidae. Exploration du Parc National Albert. Mission G. F. De Witte, 1933–1935. Fascicule 88. Institut des Parcs Nationaux de Congo Belge, Tervuren, 57pp.

Benoît, P.L.G., 1986. Bethylidae africains (Hymenoptera): V. le genre Trichiscus Benoît. Rev. Zool. Afr. 99, 293– 297.

Carr, M., Young, J.P.W. & Mayhew, P.J., 2010. Phylogeny of bethylid wasps (Hymenoptera: Bethylidae) inferred from 28S and 16S rRNA genes. Insect Syst. Evol. 41, 55–73.

Carpenter, J.M., 1999. What do we know about chrysidoid (Hymenoptera) relationships? Zool. Scr. 28, 215–231.

Evans, H.E., 1955 [1954]. The North American species of *Dissomphalus* (Hymenoptera, Bethylidae). Proc. Entomol. Soc. Wash.56, 288–309.

Evans, H.E., 1958. The North and Central American species of *Propristocera* (Hymenoptera: Bethylidae). Proc. Entomol. Soc. Wash. 59, 289–296.

Evans, H.E., 1963. A revision of the genus *Pristocera* in the Americas (Hymenoptera, Bethylidae). Bull. Mus. Comp. Zool. 129, 241–290.

Evans, H.E., 1964. A synopsis of the American Bethylidae (Hymenoptera, Aculeata). Bull. Mus. Comp. Zool. 132, 1–222.

Evans, H.E., 1969. A revision of the genus *Epyris* in the Americas (Hymenoptera, Bethylidae). T. Am. Entomol. Soc. 95, 181–352.

Evans, H.E., 1978. The Bethylidae of America North of Mexico. Mem. Am. Entomol. Inst. 27, 1– 332.

Gobbi, F.T., Azevedo, C.O., 2010. Taxonomia de *Pseudisobrachium* (Hymenoptera, Bethylidae) da Mata Atlântica Brasileira. Rev. Bras. Entomol. 54, 173–224.

Gobbi, F.T., Azevedo, C.O., 2016. Revision of *Calobrachium* Gobbi & Azevedo, gen. nov. Hymenoptera, Bethylidae), with description of seven new Oriental species. Zootaxa 4083, 221–238.

Haliday, A.H., 1839. Hymenoptera Britannica, Part 1. Oxyura. Addendum to Vol. 1. Hymenopterorum synopsis ad methodum fallenii utplurimum accomodata. Hippolytus Bailliere, London.

Harris, R. A. 1979. A glossary of surface sculpturing. Occas. Pap. Entomol. 28, 1–31.

Hebert, P.D.N., Cywunska, A., Ball, S.L., Waard, J.R., 2003. Biological identifications through DNA barcodes. Proc. R. Soc. Lond., B, Biol. Sci. 270, 313–321.

Huelsenbeck, J.P., Ronquist, F., 2001. MRBAYES: Bayesian inference of phylogenetic trees. Bioinformatics 17, 754–755.

Katoh, S., 2013. MAFFT multiple sequence alignment software version 7: improvements in performance and usability. Mol. Biol. Evol. 30, 772–780.

Kawada, R., Buffington, M.L., 2016. A Scalable and Modular Dome Illumination System for Scientific Microphotography on a Budget. PLoS ONE. 11, e0153426.

Kawada, R., Lanes, G.O., Azevedo, C.O., 2015. Evolution of metapostnotum in flat wasps (Hymenoptera, Bethylidae): implications for homology assessments in Chrysidoidea. PLoS ONE. 10, e0140051.

Lanfear, R., Calcott, B., Ho, S.Y.W., Guindon, S., 2012. Partition-Finder: combined selection of partitioning schemes and substitution models for phylogenetic analyses. Mol. Biol. Evol. 29, 1695–1701.

Lanfear R., Frandsen, P.B., Wright, A.M., Senfeld, T., Calcott, B., 2016 PartitionFinder 2: new methods for selecting partitioned models of evolution for molecular and morphological phylogenetic analyses. Mol. Biol. Evol. 34, 772–773.

Martinelli, A.B, Waichert, C., Barbosa, D.N., Fagundes, V., Azevedo, C.O., 2017. The use of Proteinase K to access genitalia morphology, vouchering and DNA extraction in minute wasps. An. Acad. Bras. Ciê. 89, 1629–1633.

Mugrabi, D.F., Azevedo, C. O. 2013. Revision of Thai *Dissomphalus* Ashmead, 1893 (Hymenoptera, Bethylidae), with description of twenty-four new species. Zootaxa 3662, 1–73.

Mugrabi, D.F., Azevedo, C.O., 2016. Description of 91 new species of *Dissomphalus* Ashmead (Hymenoptera: Bethylidae) from New Guinea Island and surrounded areas. In: Robillard, T., Legendre, F., Villemant, C., Leponce, M. (Eds.), Insects of Mount Wilhelm, Papua New Guinea. Muséum national d'Histoire naturelle, Paris, pp. 451–564. [Mémoires du Muséum national d'Histoire naturelle; 209]

Pilgrim, E.M., Von Dohlen, C.D., Pitts, J.P., 2008. Molecular phylogenetics of Vespoidea indicate paraphyly of the superfamily and novel relationships of its component families and subfamilies. Zool Scr. 37, 539–560.

Ramos, M.S., Azevedo, C.O., 2012. Revision of *Eupsenella* Westwood, 1874 (Hymenoptera, Bethylidae). Zootaxa. 3539, 1– 80.

Ramos, M.S., Azevedo, C.O. 2019. Revisited phylogeny of Bethylinae (Hymenoptera, Bethylidae) solves basal polytomy. Insect Syst. Evol. 49, 1–51.

Sorg, M. 1988. Zur Phylogenie und Systematik der Bethylidae (Insecta, Hymenoptera, Chrysidoidea). Geol. Inst. Univ. Koeln Sonderveroeffentlichungen 63, 1–146.

Stamatakis, A., 2014. RAxML version 8: a tool for phylogenetic analysis and postanalysis of large phylogenies. Bioinformatics, 30, 1312–1313.

Tamura K., Peterson D., Peterson N., Stecher G., Nei M., Kumar S., 2011. MEGA5: Molecular Evolutionary Genetics Analysis using Maximum Likelihood, Evolutionary Distance, and Maximum Parsimony Methods. Mol. Biol. Evol. 28, 2731–2739.

Tamura, K., Stecher, G., Peterson, D., Filipski, A., Kumar, S., 2013. MEGA6: Molecular Evolutionary Genetics Analysis version 6.0. Mol. Biol. Evol. 30, 2725–2729.

Terayama, M., 1995. Discovery of the genus *Protisobrachium* Benoît 1957 from the Oriental region (Hymenoptera: Bethylidae). J. Entomol. Sci. 30, 443–446.

Terayama, M., 1996. The phylogeny of the bethylid wasp subfamily Pristocerinae (Hymenoptera, Bethylidae). Jpn. J. Entomol. 64, 587–601.

Terayama, M., 2003. Phylogenetic Systematics of the family Bethylidae (Insecta: Hymenoptera) Part I. Higher Classification. Acad. Rep. Fac. Eng. Tokyo Polytech. Univ. 26, 1–14.

Waichert, C., Azevedo, C.O., 2004. Fourteen new Species of *Pseudisobrachium* (Hymenoptera, Bethylidae) from Atlantic Rain Forest of Espírito Santo, Brazil. Zootaxa 661, 1–22.

Waichert, C., Von Dohlen, C.D., Pitts, J.P., 2014. Resurrection, revision and molecular phylogenetics of Eragenia Banks with implications for Ageniellini systematics (Hymenoptera: Pompilidae). Syst. Entomol. 40, 291–321.

Xia, X. & Xie, Z., 2001. DAMBE: Data analysis in molecular biology and evolution. J. Herad. 92, 371–373.

Zamprogno, L.N., Azevedo, C.O., 2014. Phylogeny and reclassification of *Pristocera* Klug (Hymenoptera: Bethylidae). Insect Syst. Evol. 45, 1–49.

7. TABLES AND FIGURES

Table 1. Terminal taxa of phylogenetic analysis.

SPECIES	COI	28S	LW	POL2	EFALFA2	COLECTION	LOCALITY
Acrenesia sp1 DFM158	X	X	X			IBES	**PANAMA:** Darien, Cana, Serrania de Pirre, 1450 m, 4–7.VI.1996, J. Ashe & R. Brooks, flight intercept trap
Acrenesia sp2 ISA213	MG760754	MG760805	X	X		UFES	**BRASIL:** Minas Gerais, Alto Caparaó, Parque Nacional do Caparaó, 1465m, 20º30'05"S 41º49'16"W, 7.14–iii.2013, Malaise 19, C.O. Azevedo & F.B. Fraga col.
Acrenesia sp3 ISA298	MG760756	MG760807			X	CZMA	**BRASIL:** Piauí, Guaribas, PARNA Serra das Confusões, Andorinhas, 515m, 09º08'27.8"S 43º33'42.1"W, Armadilha Malaise, 01–10.ix.2013, J.A. Rafael, F. Limeira-de-Oliveira, T.T.A. Silva cols.
Acrenesia sp4 ISA300	MG760758	MG760809	X		X	CZMA	**BRASIL:** Maranhão, Carolina, PARNA Chapada das Mesas, Riacho Estiva, 265m, 07º06'59.8"S 47º21'21"W, 15–30.vi.2013, Armadilha Suspensa d'água
Acrenesia sp10 ISA12	MG760753	MG760804				UFES	**BRASIL:** Espírito Santo, Ibitirama, Parque Nacional do Caparaó, trilha da Toca de São Jorge, 1230m, 20º27'57"S 41º44'42"W, Malaise 35, 16.23.iii.2013, C.O. Azevedo & F.B. Fraga col.
Acrenesia sp12 ISA291	MG760755	MG760806				UFES	**BRASIL:** Espírito Santo, Sooretama, ReBio Sooretama, 11–19.xi.2011; M.T.; C. O. Azevedo col.
Acrenesia sp14 ISA299	MG760757	MG760808				CZMA	**BRASIL:** Piauí, Guaribas, PARNA Serra das Confusões Andorinha, 515m, 09º08'27.8"S 43º33'42.1"W, Armadilha Malaise, 01–10.i.2014, J.A. Rafael, F. Limeira-de-Oliveira, T.L. Rocha, S. Pereira cols.
Apenesia sp1 DFM065	X	X	X		X	CASC	**MADAGASCAR:** Fianarantsoa, Parc National Befotaka-Midongy, Papango 27.7 km S Midongy-Sud, Mount Papango, 13–19 Nov 2006, 23˚50'07"S 046˚57'49"E, California Academy of Sciences, coll. B.L.Fisher et al., elev 940 m, malaise, rainforest, BLF14774
Apenesia sp2 DFM119	X	X	X		X	MNHN	**PAPUA NEW GUINEA:** Province Madang Wanang (-5.22767, 145.0797) 175m, 12–13/09/2012, coll. by Basset, understorey, FIT-WAN02-D06, P090-581
Apenesia sp3 *(Neoapenesia)* DFM121	X	X	X		X	MNHN	**PAPUA NEW GUINEA:** Province Madang Wanang 3 station (-5.22767, 145.0797) 175m, 11–12/09/2012, leg Basset, Plot 3 understorey, Malaise - MAL-WAN03-D05, P047-532
Apenesia sp3 *(Neoapenesia)* ISA236	MG760759	MG760810				MNHN	**PAPUA NEW GUINEA:** Province Madang, Mount Wilhelm 700m (-5.731961,145.2522) 700m, 30–31/10/2012, leg Keltim, Uma, Novotny, Leponce, Plot 4, understorey; Malaise - MAL-MW0700D-06/16-d06
Apenesia sp4 *(Neoapenesia)* ISA239	MG760760	MG760811				MNHN	**PAPUA NEW GUINEA:** Province Madang, Wanang 3 station (-5.22767,145.0797) 175m, 28–29/11/2012, leg Basset, Plot 1, understorey; Malaise - MAL-WAN01-D11
Apenesia sp5 (*Neoapenesia*) ISA288	MG760761	MG760812				UFES	**BRASIL:** Espírito Santo, Sooretama, ReBio Sooretama, 11–19.xi.2011, M.T., C. O. Azevedo col.
Apenesia sp6 (*Neoapenesia*) ISA290	X					UFES	**BRASIL:** Espírito Santo, Sooretama; ReBio Sooretama, 11–19.xi.2011,

Austranesia sp1 ISA385	X	X	X		X	CNCI	M.T., C. O. Azevedo col. **AUSTRALIA:** Western Australia, 118km S, Exmouth on Exmouth Hwy, 55m, 22°57.5'S 113°54.6'E, 27–28.iv.2003, M.E. Irwin, FD Parker, WA-36 Malaise along road, AMNH IZC 109819
Austranesia sp1 ISA386	X	X	X		X	CNCI	**AUSTRALIA:** Queensland, Wooroonooran Nat. Park, 500m, 17°34'06"S 145°42'21"E, 9–15.ix.2004, L. Masner, rainforest, Q-7a, YPT, AMNH IZC 109820
Austranesia sp2 DFM144		X			X	ANIC	**AUSTRALIA:** -15.817°S 124.5981°E, Northwest Kimberley, Malaise - trap asmple (7 days), Coll: M23/E2rb (27 Jan 2013) OR Edwards & RK Didham, CSIRO
Austranesia sp3 DFM145	X	X			X	ANIC	**AUSTRALIA:** -15.3137°S 125.1213°,E Northwest Kimberley, Malaise - trap asmple (4 days), Coll: M22/1R3ne (31 Jan 2013) OR Edwards & RK Didham, CSIRO
Austranesia sp16 ISA130	MG760750	MG760801				IBES	**AUSTRALIA**: Western Australia, 6–17.V.2003, Maliase trap, M E Irwin, F D Parker
Austranesia sp17 ISA136	MG760751	MG760802				IBES	**AUSTRALIA:** Western Australia, 3–16.V.2003, Maliase trap, M E Irwin, F D Parker
Austranesia sp18 ISA316	MG760752	MG760803				IBES	**AUSTRALIA:** Western Australia, Mt Augustus, Natl Park, 9 km S. Tourist Camp, malaise across small dry wash, 7/9.V.2003, M.E. Irwin, F.D. Parker, 394 m, 24°22.8'S, 116°54.2'E (GPS)
Caloapenesia sp1 A27	X	X		X	X	RMNH/QSBG	**Southeastern Asia**
Caloapenesia sp2 DFM123	X	X	X	X	X	MNHN	**PAPUA NEW GUINEA:** Province Madang, Mount Wilhelm (-5.732514, 145.2568) 700m, 04–06/11/2012, Coll. by Keltim, Uma, Novotny, Leponce, understorey, FIT-MW700-C-6/8-d11, P1119-1006
Caloapenesia sp3 DFM182	X	X	X	X	X	MNHN	**PAPUA NEW GUINEA:** Province Madang, Mount Wilhelm (-5.758978,145.1861) 2200m, 19–20/10/2012, leg Mogia, Lilip, Novotny, Leponce, Plot 1, understorey; Malaise - MAL-MW2200A-04/16-d04
Caloapenesia sp4 DOC126		X		X	X	RMNH	**VIETNAN:** 2000
Caloapenesia sp5 DOC127		X		X	X	RMNH	**C. VIETNAM:** Thua Thien Hué, 2001
Caloapenesia sp6 ISA240		MG760846		X	X	MNHN	**PAPUA NEW GUINEA:** Province Madang, Mount Wilhelm (-5.758978,145.1861) 2200m, 16–17/10/2012, leg Mogia, Lilip, Novotny, Leponce, Plot 1, understorey; Malaise - MAL-MW2200A-01/16-d01
Caloapenesia sp7 ISA241		MG760847		X	X	MNHN	**PAPUA NEW GUINEA:** Province Madang, Mount Wilhelm (-5.732514,145.2568) 700m, 31–01/11/2012, leg Keltim, Uma, Novotny, Leponce, Plot 3, understorey; Malaise - MAL-MW0700C-07/16-d07
Calobrachium luangum Gobbi and Azevedo DOC407	X					QSBG	**THAILAND:** Chiang Mai, Doi Inthanon NP checkpoint 2, 18°31.559'N 98°29.941'E, 1700m, Malaise trap, 15–22.vii.2006, Y. Areeluck leg. T73
Cleistepyris sp2 ISA211	X	X	X	X		UFES	**BRASIL:** Minas Gerais, Alto Caparaó, Parque Nacional do Caparaó, 1465m, 7.14.iii.2013, 20º30'05"S 41º49'16"W, Malaise 19, C.O. Azevedo & F.B. Fraga col.
Cleistepyris sp3 ISA208	X	X	X	X		UFES	**BRASIL:** Minas Gerais, Alto Caparaó, Parque Nacional do Caparaó, 1870m, 7.14.iii.2013, 20º28'38"S 41º49'46"W, Malaise 12, C.O. Azevedo & F.B. Fraga col.
Cleistepyris sp4 ISA218	X	X	X	X		UFES	**BRASIL:** Minas Gerais, Alto Caparaó, Parque Nacional do Caparaó, 1557m, 7.14.iii.2013, 20º29'38"S 41º49'20"W, Malaise 15, C.O. Azevedo

Cleistepyris sp5 ISA293	X	X	X	X		UFES
Cleistepyris sp6 ISA292	X	X	X	X		UFES
Cleistepyris sp7 ISA294	X	X	X	X		UFES
Cleistepyris sp8 ISA217	MG760774	MG760830		X		UFES
Cleistepyris sp9 ISA20	MG760776	MG760832		X		UFES
Cleistepyris sp10 ISA212	MG760780	MG760836	X	X		UFES
Cleistepyris sp11 ISA214	MG760775	MG760831		X		UFES
Cleistepyris sp12 ISA296	MG760775	MG760833	X	X		UFES
Dissomphalus chiangmaiensis Terayama ABM171	X		X	X		QSBG
Dissomphalus chiangmaiensis Terayama ABM178	X		X	X		QSBG
Dissomphalus chiangmaiensis Terayama ABM188	X		X	X		QSBG
Dissomphalus gionus Mugrabi and Azevedo DFM101		X	X	X	X	UFES
Dissomphalus guttus Azevedo DFM110	X	X	X	X	X	IBES
Dissomphalus jubus Mugrabi and Azevedo DFM088		X	X	X	X	QSBG
Dissomphalus sp5 ABM309		X	X	X	X	MNHN
Dissomphalus turinus Mugrabi and Azevedo DFM086	X	X	X	X	X	QSBG
Dracunesia sp1 ISA198	X	X		X	X	CASC

& F.B. Fraga col.

BRASIL: Espírito Santo, Sooretama, Reserva Biol. de Sooretama, 19º00'11"S 40º07'08"W, Arm Malaise, 12–19.XI.2014, C.O Azevedo col.

BRASIL: Espírito Santo, Sooretama, Reserva Biol. de Sooretama, 19º00'11"S 40º07'08"W, Arm Malaise, 12–19.XI.2014, C.O Azevedo col.

BRASIL: Espírito Santo, Sooretama, Reserva Biol. de Sooretama, 19º00'11"S 40º07'08"W, Arm Malaise, 12–19.XI.2014, C.O Azevedo col.

BRASIL: Minas Gerais, Alto Caparaó, Parque Nacional do Caparaó, 1557m, 7.14.iii.2013, 20º29'38"S 41º49'20"W, Malaise 15, C.O. Azevedo & F.B. Fraga col.

BRASIL: Espírito Santo, Divino de São Lourenço, Parque Nacional do Caparaó, trilha do Facão de Pedra, 1500m, 20º24'30"S 41º47'06"W, Malaise 22,15.22.iii.2013, C.O. Azevedo & F.B. Fraga col.

BRASIL: Minas Gerais, Alto Caparaó, Parque Nacional do Caparaó, 1465m, 7.14.iii.2013, 20º30'05"S 41º49'16"W, Malaise 19, C.O. Azevedo & F.B. Fraga col.

BRASIL: Minas Gerais, Alto Caparaó, Parque Nacional do Caparaó, 1465m, 7.14.iii.2013, 20º30'05"S 41º49'16"W, Malaise 19, C.O. Azevedo & F.B. Fraga col.

BRASIL: Espírito Santo, Sooretama, Reserva Biol. de Sooretama, 19º00'11"S 40º07'08"W, Arm Malaise, 12–19.XI.2014. C.O Azevedo col.

THAILAND: Nakhon Si Thammarat, Namtok Yong NP, Behind campground lavatory, 8°10.434'N 99°44.508'E, 80m, Malaise trap, 12–19.viii.2008, U.prai.K. leg., T3080

THAILAND: Chiang Mai, Doi Phahompok NP, Kiewlom1: Montane Forest, 20°3.455'N 99°8.551'E, 2174m, Malaise trap, 7–14.ix.2007, Komwuan Srisom & Prasit Wongchai leg., T2810

THAILAND: Sakon Nakhon, Phu Phan NP, Creek at entrance of Huay Nam Pung Forest unit, 16°54.63'N 103°54.266'E, 281m, Malaise trap, 13–19.xi.2006, Winlon Khongnara leg., T1097

UNITED ARAB EMIRATES: Wadi Bih dam, 25.48°N 56.04°E, 30.04-04.06.2008, light trap, A. van Harten, UAE 9744

PERU: San Martín Prov, 23 km S Picota Concervación Mun. Zona Barreal, 335m, 7–14.III.2005, 7°04.88'S 76°18.89'W, ME Irwin, JD Vaquez, Malaise in tropical deciduous forest [PE 11-02]

THAILAND: Ubon Ratchathani , Pha Taem NP, Irrigation area entrance to Huay Pok forest unit, 15°37.321'N 105°36.982'E, 419m, Malaise trap, 13–20.x.2006, T722

MOZAMBIQUE: Nhica, “Ligne 34", 20–27.XI.2009, Claire Villemant rec, S 10˚42,252' E 40˚13,352', Malaise M6

THAILAND: Chiang Mai, Doi Phahompok NP, Kiewlom1: Montane Forest, 20°3.455'N 99°8.551'E, 2174m, Malaise trap, 7-14.x.2007, Komwuan Srisom & Prasit Wongchai leg., T2815

MADAGASCAR: Tulear, Province, Berenty Special, Reserve, elev 85 m, 8 km NW Amboasary, 24 March – 3 April 2003, 25°00.40' S 46°18.20' E, California Acad of Sciences, colls: M. Irwin, F. Parker, R.

Dracunesia sp2 ISA209	MG760748	MG760799		X	X	UFES	Harin'Hala, malaise trap, gallery forest, MA-02-22-20
Dracunesia sp3 ISA210	MG760749	MG760800		X	X	UFES	**BRASIL:** Minas Gerais, Alto Caparaó, Parque Nacional do Caparaó, 1465m, 20º30'05"S 41º49'16"W, 7.14.iii.2013, Malaiseb 19, C.O. Azevedo & F.B. Fraga col.
Dracunesia sp19 ISA11	MG760747	MG760798		X	X	UFES	**BRASIL:** Minas Gerais, Alto Caparaó, Parque Nacional do Caparaó, 1465m, 20º30'05"S 41º49'16"W, 7.14.iii.2013, Malaise 19, C.O. Azevedo & F.B. Fraga col.
Eleganesia sp1 DFM073	X	X	X	X		QSBG	**BRASIL:** Espírito Santo, Ibitirama, Parque Nacional do Caparaó, trilha da Toca de São Jorge, 1230m, 20º27'57"S 41º44'42"W, 16.23.iii.2013, Malaise 40, C.O. Azevedo & F.B. Fraga col.
Eleganesia sp2 DFM077			X	X		QSBG	**THAILAND:** Nakhon Ratchasima, Khao Yai NP, Moist evergreen forest at Dan chang, 14°28.285'N 101°22.57'E, 751m, Malaise trap, 19–23.xii.2006, Wirat Sook kho leg., T1310
Eleganesia sp7 ISA92		MG760827		X		QSBG	**THAILAND:** Chiang Mai, Doi Inthanon NP checkpoint 2, 18°31.559'N 98°29.941'E, 1700m, Malaise trap, 8–15.vii.2006, Y. Areeluck leg., T67
Eleganesia sp8 ISA93		MG760829		X		QSBG	**THAILAND:** Chaiyaphum, Pa Hin Ngam NP, ecotone between mix deciduous and dipterocarp forest, 15°38.132'N 101°23.922'E, 698m, Malaise trap, 19–25.ii.2007, Katae Sa-nog & Buakaw Adnafai leg., T1652
Eleganesia sp9 ISA94		MG760828		X		QSBG	**THAILAND:** Chaiyaphum, Pa Hin Ngam NP, ecotone between mix deciduous and dipterocarp forest, 15°38.132'N 101°23.922'E, 698m, Malaise trap, 19–25.ii.2007, Katae Sa-nog & Buakaw Adnafai leg., T1652
Foenobethylus sp1 DFM067	X	X	X	X	X	CASC	**THAILAND:** Chaiyaphum, Pa Hin Ngam NP, ecotone between mix deciduous and dipterocarp forest, 15°38.132'N 101°23.922'E, 698m, Malaise trap, 19–25.ii.2007, Katae Sa-nog & Buakaw Adnafai leg., T1652
Foenobethylus sp2 ISA273	MG760762	MG760813				UQIC	**SEYCHELLES:** Mahé Island, Mont Copolia, elev 520 m, 8–11 Feb 2010, 04°39'04" S 055°27'30" E, California Acad of Sciences, coll. B.L.Fisher et al., malaise trap in forest, collection code: BLF24027
Foenobethylus emiliacasellae Varkonyi and Polaszek DOC238		X		X	X	QSBG	**AUSTRALIA:** 51083
Foenobethylus emiliacasellae Varkonyi and Polaszek GU213952		MG760815/GU213952		X	X	QSBG	**THAILAND:** Kanchanaburi, Khuean Srinagarindra NP, Behind tourist center, 14°38.155'N98°59.85'E, 210m, Malaise trap, 28.viii-4.ix.2008, Chatchawan & Boonkam leg., T3422
Foenobethylus bidentatus Varkonyi and Polaszek DOC242		MG760814		X	X	QSBG	**THAILAND**
Genus A sp1 DFM062		X	X	X		CASC	**THAILAND:** Chiang Mai, Doi Chiang Dao WS Nature trail, 19°24.278'N 98°55.311'E, 491m, Malaise trap, 10–17.iii.2008, Songkran & Apichart leg., T3155
Genus B sp1 ABM298	X	X	X		X	MNHN	**MADAGASCAR:** Province Fianarantsoa, Miandritsara, Forest, 40 km S Ambositra, 20°47.56'S 47°10.54' E, 9–20 May 2005, California Acad of Sciences, coll: M. Irwin, R. Harin'Hala, malaise trap in low altitude rainforest, elev 825m, MA-29-16
							MOZAMBIQUE: Nhica, "Ligne 34", 20–27.XI.2009, Claire Villemant rec, S 10º42,456'E 40°12,518', Alt. 41 m, Malaise M1

Genus B sp1 ABM302	X	X	X		X	MNHN	**MOZAMBIQUE**: Nhica, “Ligne 34", 20–27.XI.2009, Claire Villemant rec, S 10°42,456'E 40°12,518', Malaise M6
Genus B sp2 ABM299	X	X	X		X	MNHN	**MOZAMBIQUE:** Nhica, “Ligne 34", 20–27.XI.2009, Claire Villemant rec, S 10º42,456'E 40º12,518', Alt. 92 m, Malaise M2
Genus B sp2 ABM305	X	X	X		X	MNHN	**MOZAMBIQUE:** Nhice, “Ligne 34", 20–27.XI.2009, Claire Villemant rec, S 10°42,460'E 40°12,455', Alt. 33m, Malaise M5
Genus B sp2 ABM306	X	X	X		X	MNHN	**MOZAMBIQUE:** Nhice, “Ligne 34", 20–27.XI.2009, Claire Villemant rec, S 10°42,372'E 40°13,050', Alt. 71m, Malaise M3
Genus B sp3 DFM035	X	X			X	NMKE	**KENYA:** Coast Prov. Gede Forest, 19 m, 3.30946ºS 40.01941ºE, Malaise trap, indigenous secondary growth forest, 11 sept–03 oct 2011, R. Copeland
Genus D DFM019	X	X			X	NMKE	**KENYA:** Coast Prov., Diani Beach area, 10 m, 4.27559ºS 39.59337ºE, Malaise trap, shrubland off Diani Beach Rd., 12–26 Dec 2013, R. Copeland
Parascleroderma sp1 DFM021	X		X			NMKE	**KENYA:** Coast Prov. Kasigau Mtn., indigenous forest, 1117 m, 3.82667°S 38.64982°E, Malaise trap, next to spring in forest, 21 sept–05 oct 2011, R. Copeland
Parascleroderma sp2 DFM060	X	X				CASC	**MADAGASCAR:** Majunga, Beabolay Bamboo Forest, 10 km SW of Soalala, 4 km from Baly village, 26 Sept–4 Oct 2007, 16°2.72'S 45°48.24'E, Calif Acad of Sciences, coll: M.Irwin, R.Harin'Hala, malaise in bamboo forest, elev 30 ft, MG-39A-02
Parascleroderma sp3 (*Ceratepyris*) ISA413	X	X	X			MNHN/IBES	**FRANCE:** MNHN37
Parascleroderma sp5 ISA312	MG760763	MG760816				UFES	**AUSTRALIA:** Western Australia, 74 km S, Newman on Great Northern Hwy, malaise in wash with drying pools, 6/18.V.2003, M.E. Irwin, F.D. Parker, 631 m, 23°56.0'S 19°46.0'E (GPS)
Parascleroderma sulcatifrons Kieffer DFM097	X	X	X			UFES	**UNITED ARAB EMIRATES:** Wadi Wurayah, 25.24°N 56.17°E, 11–18.05.2007, Malaise trap, A. van Harten, UAE 7900
Parascleroderma sulcatifrons Kieffer ABM288	X	X	X			MNHN/IBES	**FRANCE:** Malaucène, Mt. Vientoux, Malaise, 30.VI–7.VII.1998
Pristepyris sp1 ISA256	X	X	X	X	X	QSBG	**THAILAND:** Ubon Ratchathani, Pha Taem NP, entrance of Huay Pok substation, 15°37.21'N 105°36.918'E, 438m, Malaise trap, 25.iv–2.v.2007, Bunlu Sapsiri leg., T2172
Pristepyris sp2 ISA260	MG760740	MG760791	X	X	X	QSBG	**THAILAND:** Ubon Ratchathani, Pha Taem NP, west of Huay Pok substation, 15°37.212'N 105°36.903'E, 438m, Malaise trap, 25.iv–2.v.2007, Bunlu Sapsiri leg., T2173
Pristepyris sp3 ISA328	X	X	X	X	X	QSBG	**THAILAND:** Phitsanulok, Thung Salaeng Luang NP, Deciduous forest, 16°50.699'N 100°51.266'E, 501m, Malaise trap, 8–15.iv.2007, Pongpitak & Pranee & Sathit leg. T2399
Pristepyris sp4 ISA353	X	X	X	X	X	IBES	**USA:** Tennessee, Rhea Co., Dayton, A. P.: Hs al., 13.X.14 (04)
Pristepyris sp5 ISA355	X	X	X	X	X	IBES	**USA:** Tennessee, Rhea Co., Dayton, A. P.: Hs al., 13.X.14 (04)
Pristepyris sp6 ISA373	X	X	X	X	X	CNCI	**USA:** Texas, Lamar Co., Camp Maxey, 30.vii–21.x.2003, W Godwin, SFASU lot 89, MT in Equisetum bog, AMNH IZC 109903
Pristepyris sp7 ISA251	MG760779	MG760835		X	X	QSBG	**THAILAND:** Ubon Ratchathani, Pha Taem NP Phu Krajeaw foothill,

Pristepyris sp8 ISA352	MG760746	MG760797	X	X	X	IBES	**USA:** Tennessee, Rhea Co., Dayton, A. P.: Hs al., 13.X.14 (04)
Pristepyris sp9 ISA266	MG760739	MG760790		X	X	QSBG	**THAILAND:** Nakhon Nayok, Khao Yai NP Lum Ta Kong View Point, 14°25.565'N 101°23.442'E, 726m, Malaise trap, 26.iv–2.v.2007, Pong Sandao leg. T2130
Pristocera sp1 ABM51	MG760772	MG760825			X	UFES	**UNITED ARAB EMIRATES**
Pristocera sp2 ABM316	X	X	X		X	MNHN	**MOZAMBIQUE:** Lle de Vamizy, S 11˚01,465' E 40˚40,985', Alt. 10m, Malaise P2, 28–30.XI.2009, Claire Villemant rec
Pristocera sp3 ISA252	MG760770	MG760823	X		X	QSBG	**THAILAND:** Ubon Ratchathani, Pha Taem NP Phu Krajeaw foothill, 15°39.989'N 105°30.468'E, 238m, Malaise trap, 2–9.vi.2007, Tongcam & Banlu leg., T2206
Pristocera sp4 ISA342	X	X	X		X	YNU	**SOUTH KOREA:** [DG] Dalseo-gu Daegok-dong Daegu Arboretum / N35°47'48.6" E128°31'33.5" (alt 88m) / 2012.ix.5–ix.9 Coll Sing-Gu Kang
Pristocera sp5 ISA368	X	X			X	IBES	**MADAGASCAR:** MA-01 9A (76)
Pristocera sp6 ISA395	X	X	X		X	AMNH	**REPUBLIC OF GHANA:** Bobiri Forest Reserve, 06°42'N 01°20'W, 23–31.vii.2001, Chris Carlton, FIT, AMNH IZC 109947
Pristocera sp7 DFM047	X	X			X	CASC	**MADAGASCAR:** Province Antsiranana, Marojejy Nat'l Park, 5 km W Manantenina village, Camp Mantella, 18–25 March 2005, 14°26.29'S 49°46.44'E, California Acad of Sciences, coll: M. Irwin, R. Harin'Hala, malaise trap, low altitude, rainforest, elev. 490 m, MA-31-16
Pristocera sp8 DFM114	X	X	X		X	IBES	**MADAGASCAR:** Ranomafana, 01-19.X.2002, MA-02-04B-40
Pristocera sp9 (*Dicrogenium*) ISA22	X	X	X		X	ISAM	**UGANDA:** UG08-KF2M12
Pristocera sp10 (*Dicrogenium*) ABM310	X	X	X		X	MNHN	**MOZAMBIQUE:** Nhica, “Ligne 34", 20–27.XI.2009, Claire Villemant rec, S10˚42,252' E40˚13,352', Malaise M6
Pristocera sp11 (*Dicrogenium*) ABM303	X	X			X	MNHN	**MOZAMBIQUE:** Nhice, “Ligne 34", 20–27.XI.2009, Claire Villemant rec, S10˚42,460' E40˚12,455', Alt. 33m, Malaise M5
Pristocera sp12 ISA278	MG760741	MG760792				NMKE	**KENYA:** 18
Pristocera sp13 ISA284	MG760742	MG760793				NMKE	**KENYA:** 13
Propristocera sp2 ABM296		X	X		X	MNHN	**MOZAMBIQUE:** Nhica, “Ligne 34", 20–27.XI.2009, Claire Villemant rec, S10º42,456'E 40º12,518', Alt. 41 m, Malaise M1
Propristocera sp3 ABM304	X	X	X		X	MNHN	**MOZAMBIQUE:** Nhice, “Ligne 34", 20–27.XI.2009, Claire Villemant rec, S10º42,460'E 40º12,455', Alt. 33m, Malaise M5
Propristocera sp4 DFM017	X	X			X	NMKE	**KENYA:** Eastern Prov., Simisi area, 2.05111ºS 38.32613ºE, 710 m, Malaise trap at base of Yamalu Hill, Acacia shrubland, 28 nov–01 dec 2013, R. Copeland
Propristocera sp5 DFM024		X			X	NMKE	**KENYA:** Coast Prov. Kaya Kinondo, indigenous forest, 4.39618ºS 39.54582ºE, 5 m, Malaise trap, coral rag canopy forest, 11–25 dec 2011, R. Copeland
Propristocera sp6 ISA76	X	X			X	QSBG	**THAILAND:** Chiang Mai, Doi Phahompok NP, Kiewlom1: Montane Forest, 20°3.455'N 99°8.551'E, 2174m, Malaise trap, 7–14.ix.2007, Komwuan Srisom & Prasit Wongchai leg., T2810
Propristocera sp7 ISA267	X				X	QSBG	**THAILAND:** Ubon Ratchathani, Pha Taem NP, Foot of Phu Kra jeaw, 15°39.989'N 105°30.468'E, 238m, Malaise trap, 4–11.xii.2006,

Propristocera sp8 ISA279	MG760744	MG760795	X		X	NMKE	**KENYA:** 18
Propristocera sp9 ISA336	MG760745	MG760796	X		X	QSBG	**THAILAND:** Phitsanulok, Thung Salaeng Luang NP, Dry Evergreen forest, 16°50.277'N 100°52.917'E, 486m, Malaise trap, 8–15.iv.2007, Pongpitak & Pranee & Sathit leg., T2397
Propristocera sp23 ISA249	MG760743	MG760794			X	QSBG	**THAILAND:** Ubon Ratchathani, Pha Taem NP, Huay Pok waterfall, 15°37.321'N 105°36.982'E, 419m, Malaise trap, 18–25.iv.2007, Bunlu Sapsiri leg., T2171
Protisobrachium sp1 A76	MG760767	MG760820		X		CASC	**MADAGASCAR**
Protisobrachium sp2 DFM025		X		X		NMKE	**KENYA:** Coast Prov. Kaya Kinondo, indigenous forest, 4.39618ºS 39.54582ºE, 5 m, Malaise trap, coral rag canopy forest, 11–25 dec 2011, R. Copeland
Protisobrachium sp3 DFM027		X		X		NMKE	**KENYA:** Coast Prov. Taita Hills, Ngangao Forest, 3.36100ºS 38.34186ºE, 1848 m, Malaise trap, indigenous forest, 18 sept–02 oct 2011, R. Copeland
Protisobrachium sp3 DFM037	X	X		X		NMKE	**KENYA:** Coast Prov. Taita Hills, Vuria Forest, 3.41428ºS 38.29178ºE, 2162 m, Malaise trap, just inside indigenous forest, 22 feb–08 mar 2012, R. Copeland
Protisobrachium sp4 DFM039	X	X		X		NMKE	**KENYA:** Rift Valley Prov., Nguruman, nr. Sampu River, 723 m, 1.90117ºS 36.05040ºE, Malaise trap, nr. base of Nguruman Escarpment, 10–24.IX.2011, R. Copeland
Protisobrachium sp5 ABM283	MG760766	MG760819		X		NMKE	**KENYA**
Pseudisobrachium sp1 DFM040		X		X		NMKE	**KENYA:** Coast Prov., Mrima Hill Forest, 212 m, 4.48576°S 39.25845°E, Malaise trap, indigenous forest, edge, 11–25 dec 2011, R. Copeland
Pseudisobrachium sp2 DFM083		X	X	X		QSBG	**THAILAND:** Ubon Ratchathani , Pha Taem NP, Huay Sa Nhom plateau, 15°27.435'N 105°34.838'E, 238m, Malaise trap , 25.xi–2.xii.2006, Sorawit and Thongdee leg., T1061
Pseudisobrachium sp3 DFM105	X	X		X		IBES	**USA:** Tennessee, Rhea Co., Dayon, A. Pitts coll., 01.IX.2014
Pseudisobrachium sp4 DFM147	X	X		X	X	CNCI	**CUBA:** Santiago Prov., Gran Piedra, 1100m , 14–17.XII.1995, L. Masner YPT
Pseudisobrachium sp5 DFM150	X			X		CNCI	**HONDURAS:** Departamento de Atlantida, Tela, Lancetilla Botanical Garden, 23 Ine 1994, 10–20 m, J. Ashe, R. Brooks # 199 ex. flight intercept trap
Pseudisobrachium sp6 DFM177	X	X	X	X	X	CZMA	**BRASIL:** MA, Carolina, PARNA Chapada das Mesas, Riacho do Sucuruiu, 240m, 07˚07'05.6"S 47˚18'31.6"W, Malaise, 20–31.VIII.2013, J.A. Rafael, F. Limeira-de-Oliveira, TTA Silva cols.
Pseudisobrachium sp7 CZMA09	X	X		X		CZMA	**BRASIL:** MA, Carolina, PARNA Chapada das Mesas, Riacho Sucuruiu, 240m, 07˚07'05.6"S 47˚18'31.6"W, Malaise, 10–20.XII.2013, J.A. Rafael, F. Limeira-de-Oliveira, TTA Silva cols.
Pseudisobrachium sp8 CZMA11	X	X	X	X		CZMA	**BRASIL:** MA, Carolina, PARNA Chapada das Mesas, Riacho Sucuruiu, 240m, 07˚07'05.6"S 47˚18'31.6"W, Malaise, 10–20.XII.2013, J.A. Rafael, F. Limeira-de-Oliveira, TTA Silva cols.
Pseudisobrachium sp9 CZMA14	MG760787	MG760843	X	X		CZMA	**BRASIL:** MA, Carolina, PARNA Chapada das Mesas, Riacho Sucuruiu, 240m, 07˚07'05.6"S 47˚18'31.6"W, Malaise, 10–20.XII.2013, J.A. Rafael, F. Limeira-de-Oliveira, TTA Silva cols.

Thongcome & Pakdee leg., T1200

Pseudisobrachium sp10 ABM61	X	X	X	X		UFES	**UNITED ARAB EMIRATES:** Wadi Bih Dam, 25.48˚N 56.04˚E, 22.02–01.03.2007, light trap, A. van Harten, UAE7592
Pseudisobrachium sp11 ABM65	X	X	X	X	X	QSBG	**THAILAND**: Loei, Phu Ruea NP Subhnonghin, 17°28.772'N 101°21.308'E, 860m, Malaise trap, 26.vii–2.viii.2006, Nukoonchai Jaroenchai leg., T319
Pseudisobrachium sp12 ABM300		X	X	X		MNHN	**MOZAMBIQUE:** Nhica, "Ligne 34", 20–27.XI.2009, Claire Villemant rec, S 10º42,456' E 40º12,518', Alt. 92 m, Malaise M2
Pseudisobrachium sp13 ABM317	X	X	X	X	X	MNHN	**MOZAMBIQUE:** Lle de Vamizy, S 11˚01,465' E 40˚40,985', Alt. 10m, Malaise P2, 28–30.XI.2009, Claire Villemant rec
Pseudisobrachium sp14 ISA360	X	X	X	X		IBES	**USA:** Tennessee, Rhea Co., Dayton, A. Pitts col., 21.ix.14 (06)
Pseudisobrachium sp15 ISA191	MG760788	MG760844		X		UFES	**BRASIL:** Minas Gerais, Alto Caparaó, Parque Nacional do Caparaó, 1557m, 20º29'38"S 41º49'20"W, 7.14.iii.2013, Malaise 15, C.O. Azevedo & F.B. Fraga col.
Pseudisobrachium sp16 ISA359	MG760789	MG760845		X		IBES	**USA:** Tennessee, Rhea Co., Dayton, A. Pitts col., 21.ix.14 (06)
Trichiscus mourei ABM19	X	X	X		X	NMKE	**KENYA:** Coast Prov. Funzi Island, near sea lavel, 4.57749˚ 39.43825˚ E, Malaise Trap, nr. Funzi workshop, 4–10 Jul.2012, Coll.: ICIPE/NMK Funzi Island Expedition. IBOL 14635BethC10. Holotype
Trichiscus sp1 A120	X		X		X	ISAM	**SOUTH AFRICA:** KwaZulu-Natal
Trichiscus jimi Azevedo ABM16		X			X	NMKE	**KENYA:** Lake Bogoria, 0˚11.7' N 36˚7.3'E, Fig Tree Campsite, Malaise Trap, 20.viii.98, R. Copeland. Paratype
Trichiscus cf *mourei* ABM90	X				X	NMKE	**KENYA**: Coast Prov., Mrima Hill Forest, 212 m, 4.48576˚S 39.25845˚E, Malaise trap, indigenous forest, edge, R. Copeland
Trichiscus cf *mourei* ABM91	X				X	NMKE	**KENYA**: Coast Prov., Mrima Hill Forest, 212 m, 4.48576˚S 39.25845˚E, Malaise trap, indigenous forest, edge, R. Copeland
Trichiscus sp2 ABM94	X		X		X	NMKE	**KENYA:** Eastern Prov., Ngaia Forest, bottom, of forest, 0.32442°N 38.05038°E, 1057 m, Malaise trap, inside, indigenous forest, R. Copeland
Trichiscus sp3 ABM95	MG760764	MG760817	X		X	NMKE	**KENYA:** Eastern Prov., Ngaia Forest, bottom, of forest, 0.32442°N 38.05038°E, 1057 m, Malaise trap, inside, indigenous forest, R. Copeland
Trichiscus sp4 ABM96	MG760765	MG760818			X	NMKE	**KENYA:** Coast Prov., Taita Hills, Mwatate area, 3.48444ºS 38.33251º E, 1011 m, Malaise trap, below Bura Bluff, riverine forest, R. Copeland
OUTGROUP							
Goniozus sp1 DOC392		X				MPEG	**BRASIL:** Pará, Juriti, Propiedade Barroso, arm. Malaise, O. T. Silveira & equipe col.
Goniozus sp2 Doc000	MG760783	MG760839				-	-
Odontepyris sp1 DOC287		X				CASC	**MADAGASCAR:** Toliara, Prov. Fiherenana, elev ? m, 23°10.619'S 43°57.685'E, 18–22 August 2003, California Acad. of Sciences, colls: Frontier Wilderness, Project, Malaise trap, in small undisturbed riparian, forest valley, MGF078
Odontepyris sp1 DOC435		X				ISAM	**SOUTH AFRICA:** KwaZulu-Natal [KZN09]
Prosierola sp1 DOC393		X				MPEG	**BRASIL:** Pará, Juriti, Mineração Alcoa, Capiranga, 30.V–03.VI2008, arm. Malaise, J. N. Santos & L. A. Quaresma col.
Prosierola sp2 DOC397	X	X				MPEG	**BRASIL:** Pará, Melgaço, Floresra Nacional Caxiuanã, Trilha Igarapé Ararua, 21.xi-26.xi.2003, arm Malaise 11, A. P. Aguiar & J. Dias, Ponto P05188
Prosierola sp2 DOC399		X				CPDC	**BRASIL:** Bahia, Ubaítaba, Faz. Fortaleza, 14°18'S 39°19'W,

					13.XII.2003, arm. Malaise
Sierola sp1 DOC260	MG760782	MG760838	X	UFES	**USA:** Hawaii, 1657
Sierola sp2 DOC261	X	X	X	UFES	**USA:** Hawaii, 1657
Sierola gracilis Fullaway DOC262	MG760781	MG760837	X	UFES	**USA:** Hawaii

Table 2. Primer sequences (written 5' to 3') used and best models selected to the nine partitions obtained for the five molecular markers.

GENE	SEQUENCE	LENTH	REFERENCE	EVOLUTIVE MODEL
COI[1]				
Forward (HCO-2198)	TAAACTTCAGGGTGACCAAAAAATCA	~620 pb	Folmer *et al.* (1994)	**1/3 -** TIM3+I+G
Reverse (LCO-1490)	GGTCAACAAATCATAAAGATATTGG		Folmer *et al.* (1994)	**2/3 -** TVM+G
				3/3 - HKY+I+G
28S[2]				
Forward (F2)	AGAGAGAGTTCAAGAGTACGTG	~635 pb	Belshaw & Quicke (1997)	GTR+I+G
Reverse (D3)	TAGTTCACCATCTTTCGGGTC		Mardulyn & Whitfield (1999)	
EF-1α[3]				
Forward (F2for1)	GGTTCCTTCAAATATGCTTGGG	~979 pb	Pilgrim *et al.* (2008)	SYM+I+G
Reverse (F2rev1)	AATCAGCAGCACCTTTAGGTGG		Danforth & Ji (1998)	
Pol II[4]				
Forward (Polfor2a)	AAYAARCCVGTYATGGGTATTGTRCA	~625 pb	Danforth *et al.* (2006)	**1/3 -** TrN+I+G
Reverse (PL758R)	ACGACCATAGCCTTBAGRTTRTTRTAYTC		Wild & Maddison (2008)	**2/3 -** TrN+I+G
				3/3 - TrN+I+G
LWRh[5]				
Forward (MutiOpsin1F)	ACGCGATGTGCGGTTCACTGTTCGG	~580 pb	Pilgrim *et al.* (2008)	TPM1uf+I+G
Reverse (LWRhR)	AATTGCTATTAYGARACNTGGGT		Mardulyn & Cameron (1999)	

[1] – Initial denaturation at 95 °C for 3 min; 44 cycles [denaturation at 95 °C for 30 s, annealing at 47 °C for 45 s and extension at 72 °C for 45 s]; and final extension at 72 °C for 5 min.

[2] – Initial denaturation at 95 °C for 3 min; 44 cycles [denaturation at 95 °C for 45 s, annealing at 55 °C for 45 s and extension at 72 °C for 45 s]; and final extension at 72 °C for 5 min.

[3] – Initial denaturation at 95 °C for 3 min; 44 cycles [denaturation at 95 °C for 45 s, annealing at 55 °C for 45 s and extension at 72 °C for 45 s]; and final extension at 72 °C for 5 min.

[4] – Initial denaturation at 95 °C for 3 min; 44 cycles [denaturation at 95 °C for 60 s, annealing at 54 °C for 1 min and extension at 72 °C for 1 min]; and final extension at 72 °C for 5 min.

[5] – Initial denaturation at 95 °C for 3 min; 44 cycles [denaturation at 95 °C for 45 s, annealing at 58 °C for 45 s and extension at 72 °C for 60 s]; and final extension at 72 °C for 5 min.

Table 3. Comparison between the morphological patterns found in *Acrenesia* large- and small-bodied styles.

Characters	***Acrenesia* large-bodied style**	***Acrenesia* small-bodied style**
Antenna, *flagelomers length*	Very Long	Long
Protorax, *Pronotal flange (in lateral view)*	Vertical	Subvertical
Anteromesoscutum, *notaulus*	Incomplete posteriorly	Complete posteriorly or nearly so
Forewing, *Junction of Rs&M and cu-a*	not angled	angled
Vannus	Narrow	Broad
Hind wing, *julgal lobe*	Regular-sized	Reduced
Hypopygium, *lateral stalk*	Far from anterior corner of hypopygium	Close to anterior corner of hypopygium
corner of anterior margin	With narrow projection	With board projection
Male genilaia, *paramere in dorsal view*	Fused to basiparamere	Outlined, just connected to basiparamere
modification of paramere	Paramere excavated basally to acommodated cuspis	Paramere not excavated
shape of paramere	Bevelled appicaly	Base narrow and apex very expanded
ventral surface of paramere	Absent	Presente
basal ring	Present	Absent
length of digitus	very large	very small


Sierola sp2 DOC261
Sierola sp1 DOC260
Sierola gracilis Fullaway DOC262
Prosierola sp2 DOC397
Prosierola sp2 DOC399
Goniozus sp2 Doc000
Prosierola sp1 DOC393
Goniozus sp1 DOC392
Odontepyris sp1 DOC287
Odontepyris sp1 DOC435
Calobrachium luangum Gobbi and Azevedo DOC407
Caloapenesia sp1 A27
Caloapenesia sp5 DOC127
Caloapenesia sp4 DOC126
Caloapenesia sp3 DFM182
Caloapenesia sp6 ISA240
Caloapenesia sp2 DFM123
Caloapenesia sp7 ISA241
Clade A
Pseudisobrachium sp6 DFM177
Pseudisobrachium sp5 DFM150
Pseudisobrachium sp3 DFM105
Pseudisobrachium sp14 ISA360
Pseudisobrachium sp16 ISA359
Pseudisobrachium sp4 DFM147
Pseudisobrachium sp13 ABM317
Pseudisobrachium sp10 ABM61
Pseudisobrachium sp12 ABM300
Pseudisobrachium sp1 DFM040
Pseudisobrachium sp2 DFM083
Pseudisobrachium sp15 ISA191
Pseudisobrachium sp11 ABM65
Pseudisobrachium sp8 CZMA11
Pseudisobrachium sp7 CZMA09
Pseudisobrachium sp9 CZMA14
Clade B
Pristocera sp12 ISA278
Pristocera sp13 ISA284
Pristocera sp9 (Dicrogenium) ISA22
Pristocera sp10 (Dicrogenium) ABM310
Pristocera sp11 (Dicrogenium) ABM303
Pristocera sp2 ABM316
Pristocera sp1 ABM51
Pristocera sp3 ISA252
Pristocera sp4 ISA342
Pristocera sp6 ISA395
Pristocera sp5 ISA368
Pristocera sp7 DFM047
Pristocera sp8 DFM114
Propristocera sp2 ABM296
Propristocera sp4 DFM017
Propristocera sp5 DFM024
Propristocera sp3 ABM304
Propristocera sp23 ISA249
Propristocera sp7 ISA267
Propristocera sp9 ISA336
Propristocera sp8 ISA279
Propristocera sp6 ISA76
Pristepyris sp3 ISA328
Pristepyris sp1 ISA256
Pristepyris sp2 ISA260
Pristepyris sp9 ISA266
Pristepyris sp7 ISA251
Pristepyris sp4 ISA353
Pristepyris sp8 ISA352
Pristepyris sp6 ISA373
Pristepyris sp5 ISA355
Clade F
Genus D DFM019
Protisobrachium sp1 A76
Protisobrachium sp3 DFM027
Protisobrachium sp3 DFM037
Protisobrachium sp4 DFM039
Protisobrachium sp5 ABM283
Protisobrachium sp2 DFM025
Dissomphalus sp5 ABM309
Dissomphalus guttus Azevedo DFM110
Dissomphalus jubus Mugrabi and Azevedo DFM088
Dissomphalus gionus Mugrabi and Azevedo DFM101
Dissomphalus turinus Mugrabi and Azevedo DFM086
Dissomphalus chiangmaiensis Terayama ABM188
Dissomphalus chiangmaiensis Terayama ABM178
Dissomphalus chiangmaiensis Terayama ABM171
Clade E (part)
Clade J
continue
Clade I

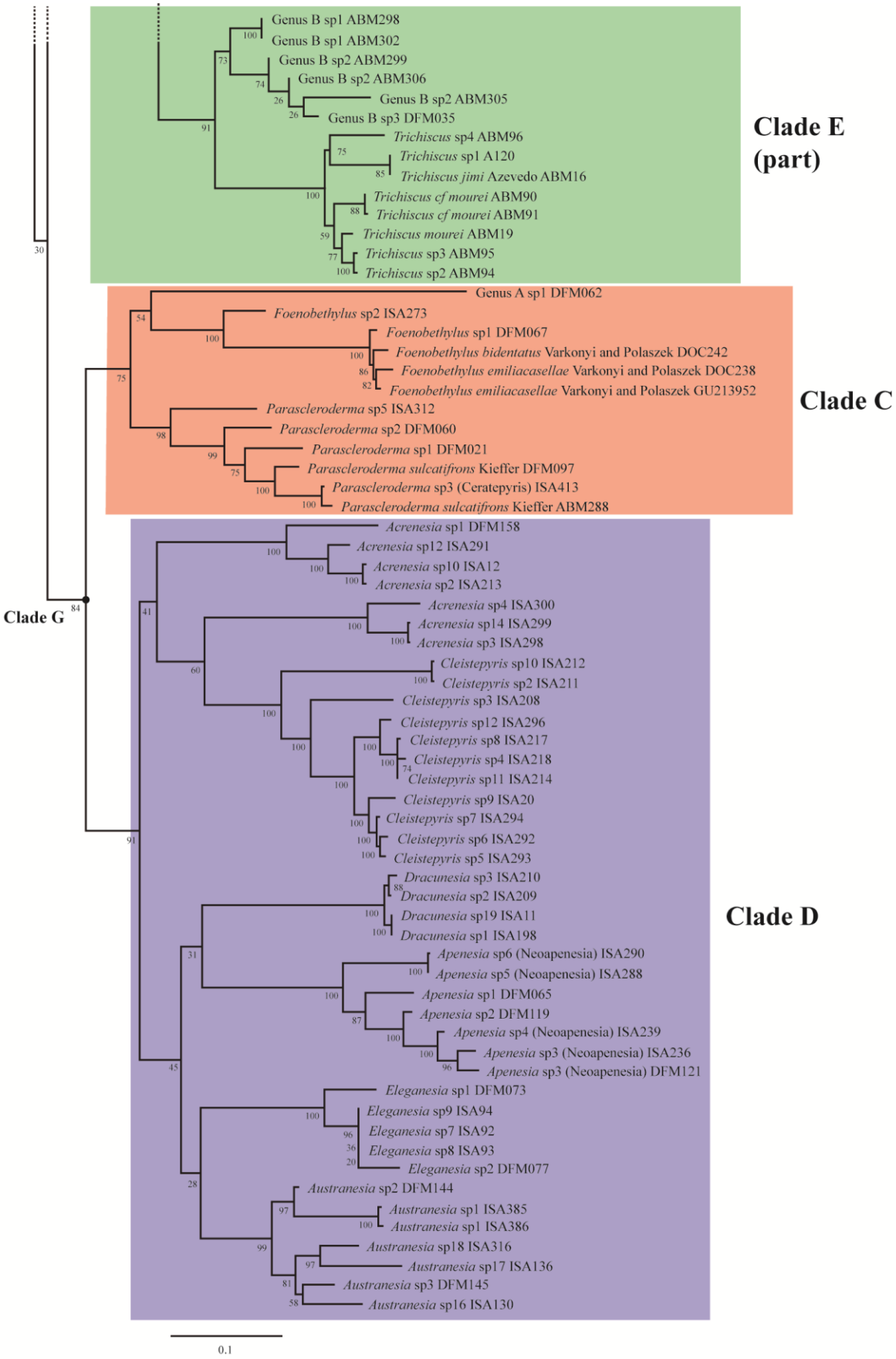

Figure 1. Maximum likelihood of Pristocerinae based on concatenated sequence data (COI, 28S, EF-1α, Pol II and LWRh). Values of bootstrap values are given next to the branches.


Sierola sp2 DOC261
Sierola gracilis Fullaway DOC262
Sierola sp1 DOC260
Odontepyris sp1 DOC287
Odontepyris sp1 DOC435
Goniozus sp1 DOC392
Goniozus sp2 Doc000
Prosierola sp1 DOC393
Prosierola sp2 DOC397
Prosierola sp2 DOC399
Calobrachium luangum Gobbi and Azevedo DOC407
Caloapenesia sp1 A27
Caloapenesia sp5 DOC127
Caloapenesia sp4 DOC126
Caloapenesia sp2 DFM123
Caloapenesia sp7 ISA241
Caloapenesia sp3 DFM182
Caloapenesia sp6 ISA240
Clade A
Pseudisobrachium sp6 DFM177
Pseudisobrachium sp14 ISA360
Pseudisobrachium sp16 ISA359
Pseudisobrachium sp4 DFM147
Pseudisobrachium sp15 ISA191
Pseudisobrachium sp8 CZMA11
Pseudisobrachium sp7 CZMA09
Pseudisobrachium sp9 CZMA14
Pseudisobrachium sp11 ABM65
Pseudisobrachium sp3 DFM105
Pseudisobrachium sp2 DFM083
Pseudisobrachium sp10 ABM61
Pseudisobrachium sp13 ABM317
Pseudisobrachium sp1 DFM040
Pseudisobrachium sp5 DFM150
Pseudisobrachium sp12 ABM300
Clade B
Genus A sp1 DFM062
Foenobethylus sp2 ISA273
Foenobethylus sp1 DFM067
Foenobethylus bidentatus Varkonyi and Polaszek DOC242
Foenobethylus emiliacasellae Varkonyi and Polaszek GU213952
Foenobethylus emiliacasellae Varkonyi and Polaszek DOC238
Parascleroderma sp5 ISA312
Parascleroderma sp2 DFM060
Parascleroderma sp1 DFM021
Parascleroderma sulcatifrons Kieffer DFM097
Parascleroderma sp3 (Ceratepyris) ISA413
Parascleroderma sulcatifrons Kieffer ABM288
Clade C
Clade G
Acrenesia sp1 DFM158
Acrenesia sp12 ISA291
Acrenesia sp10 ISA12
Acrenesia sp2 ISA213
Acrenesia sp4 ISA300
Acrenesia sp14 ISA299
Acrenesia sp3 ISA298
Cleistepyris sp10 ISA212
Cleistepyris sp2 ISA211
Cleistepyris sp3 ISA208
Cleistepyris sp12 ISA296
Cleistepyris sp11 ISA214
Cleistepyris sp4 ISA218
Cleistepyris sp8 ISA217
Cleistepyris sp9 ISA20
Cleistepyris sp7 ISA294
Cleistepyris sp5 ISA293
Cleistepyris sp6 ISA292
Dracunesia sp1 ISA198
Dracunesia sp19 ISA11
Dracunesia sp2 ISA209
Dracunesia sp3 ISA210
Apenesia sp5 (Neoapenesia) ISA288
Apenesia sp6 (Neoapenesia) ISA290
Apenesia sp1 DFM065
Apenesia sp2 DFM119
Apenesia sp4 (Neoapenesia) ISA239
Apenesia sp3 (Neoapenesia) DFM121
Apenesia sp3 (Neoapenesia) ISA236
Eleganesia sp1 DFM073
Eleganesia sp7 ISA92
Eleganesia sp8 ISA93
Eleganesia sp9 ISA94
Eleganesia sp2 DFM077
Austranesia sp2 DFM144
Austranesia sp1 ISA385
Austranesia sp1 ISA386
Austranesia sp16 ISA130
Austranesia sp3 DFM145
Austranesia sp17 ISA136
Austranesia sp18 ISA316
Clade D
continue

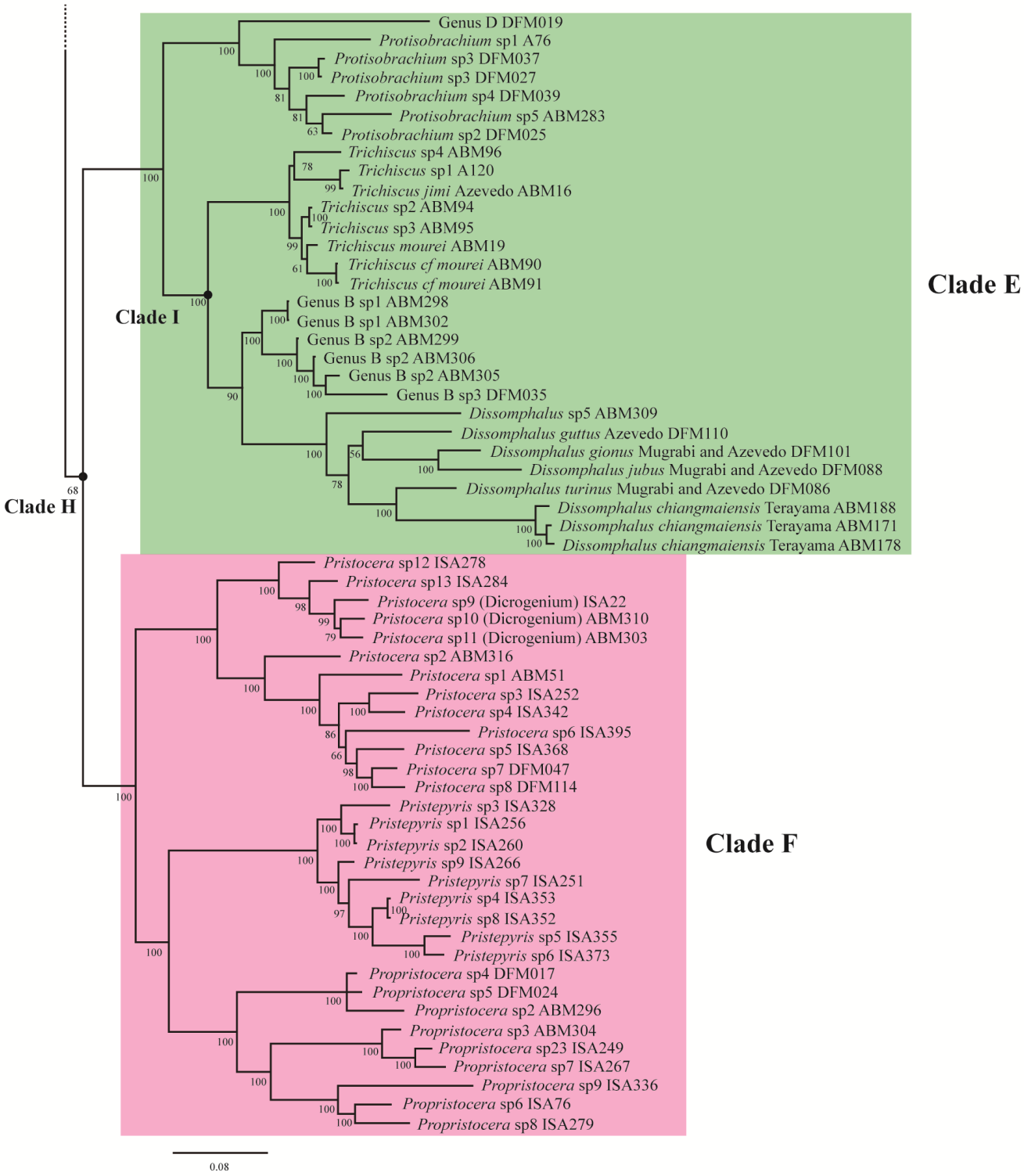

Figure 2. Phylogenetic Bayesian reconstruction of Pristocerinae based on concatenated sequence data (COI, 28S, EF-1α, Pol II and LWRh). Values of posterior probability are shown next to the branches.

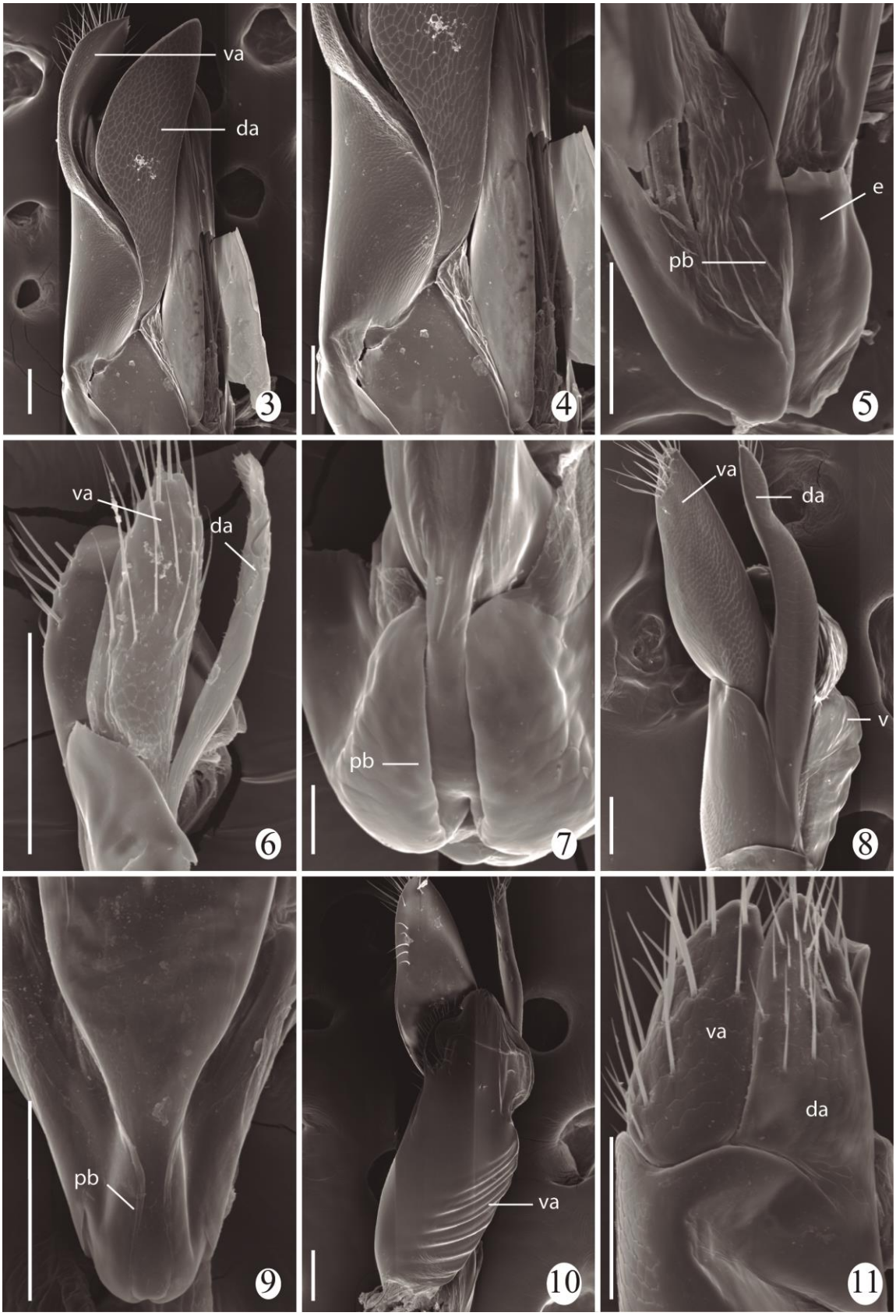

Figures 3–11. Male genitalia. 3–5. *Caloapenesia* in lateral view. 5. Sclerite of aedeagus basis (e) in dorsal. 6–7. *Calobrachium*. 6. Lateral view. 7. Dorsal view. 8–10. *Pseudisobrachium*. 8. Lateral view. 9. Dorsal view. Internal view of basiparamere. 11. *Eupsenella* in lateral view. Label: (va) ventral arm of paramere; (da) dorsal arm of paramere; (pb) projection dorsal and basal of basiparamere covering the base of aedeagus. Scale bar: 100 µm, except 7 (20 µm) and 11 (50 µm).

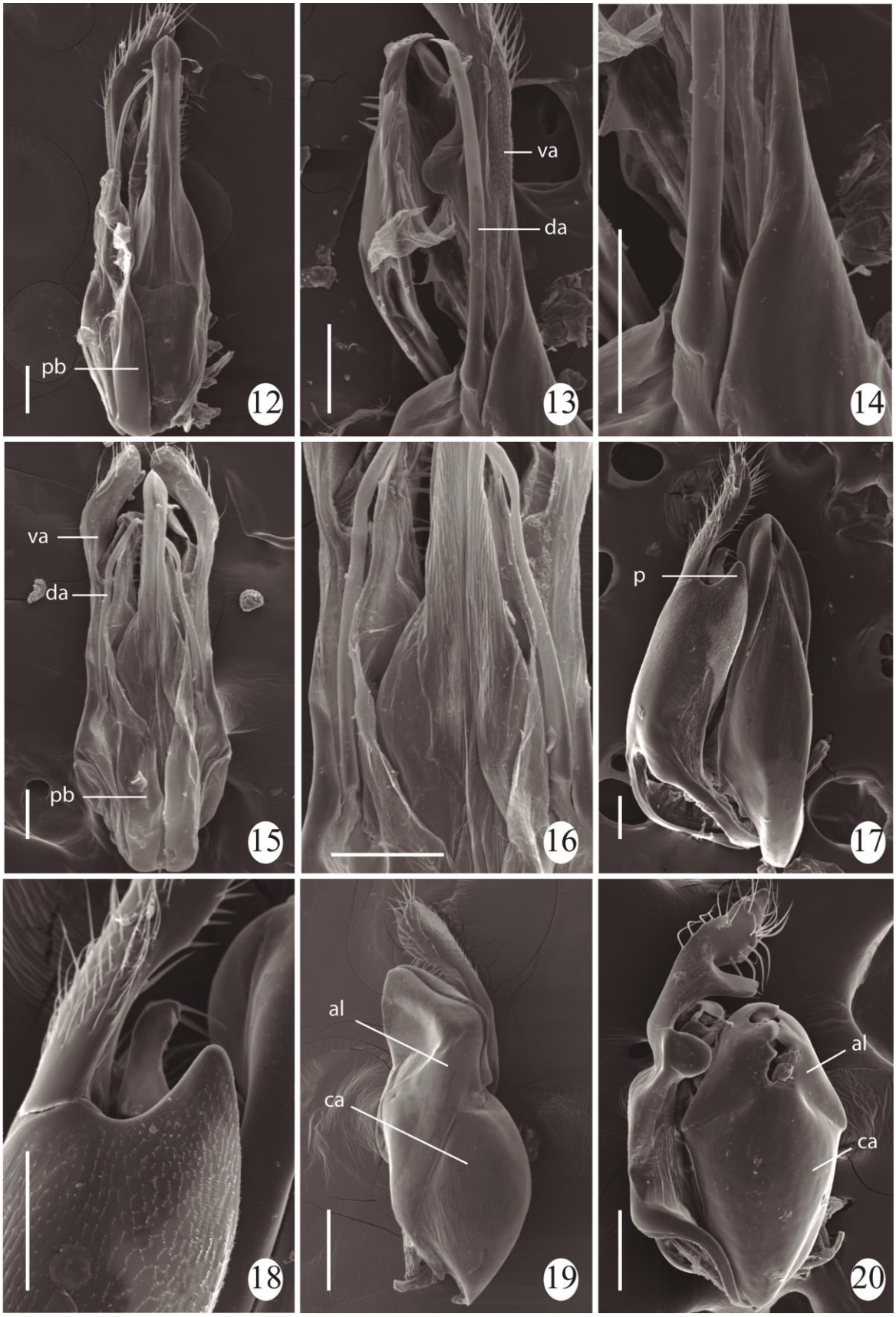

Figures 12–20. Male genitalia. 12–14. *Heterocoelia* in dorsal view. 15–16. *Zimancus* in dorsal view. 17–18. *Apenesia* in dorsal view. 19. *Parascleroderma* in lateral-dorsal view. 20. *Foenobethylus* in dorsal view. Label: (pb) projection dorsal and basal projection of basiparamere covering the base of aedeagus; (va) vental arm of paramere; (da) dorsal arm of paramere; (p) apical projection of the basiparamere; (al) laleral and apical lobe of aedeagus; (ca) central area of of aedeagus. Scale bar: 100 µm.

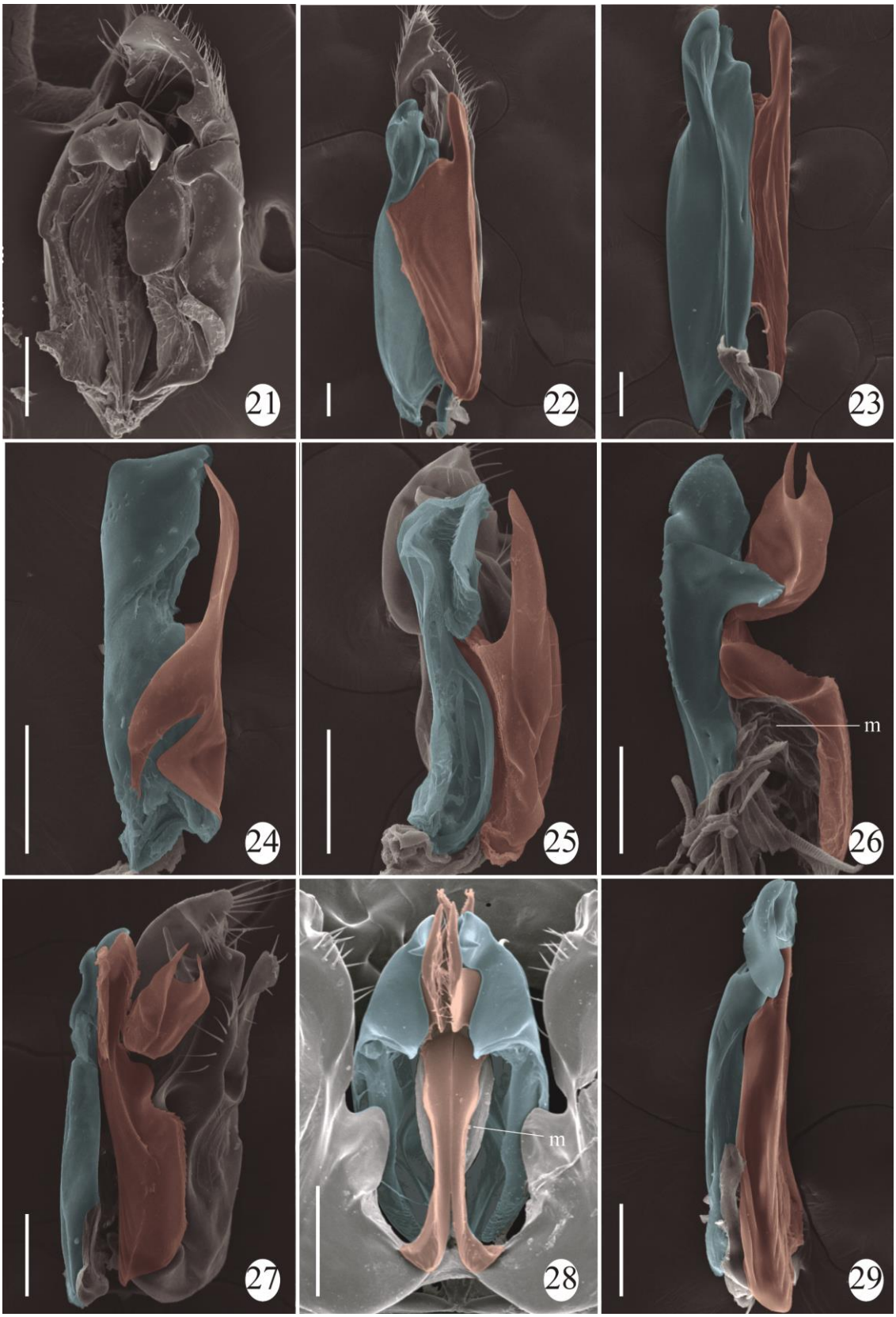

Figures 21–**29.** Male genitalia. 21. *Foenobethylus* in vetral view. 22–29. Lateral view of complex aedeagus. 22–23. *Pristepyris*. 22. External lateral face 23. Internal lateral face. 24–25. *Dissomphalus*. 24. External lateral face 25. Internal lateral face. 26–28. Genus B. 26. External lateral face 27. Internal lateral face. 28. Ventral view. 29. Genus D. 29. External lateral face. Dorsal body colored in blue, ventral ramus in red. Scale bar: 100 μm.

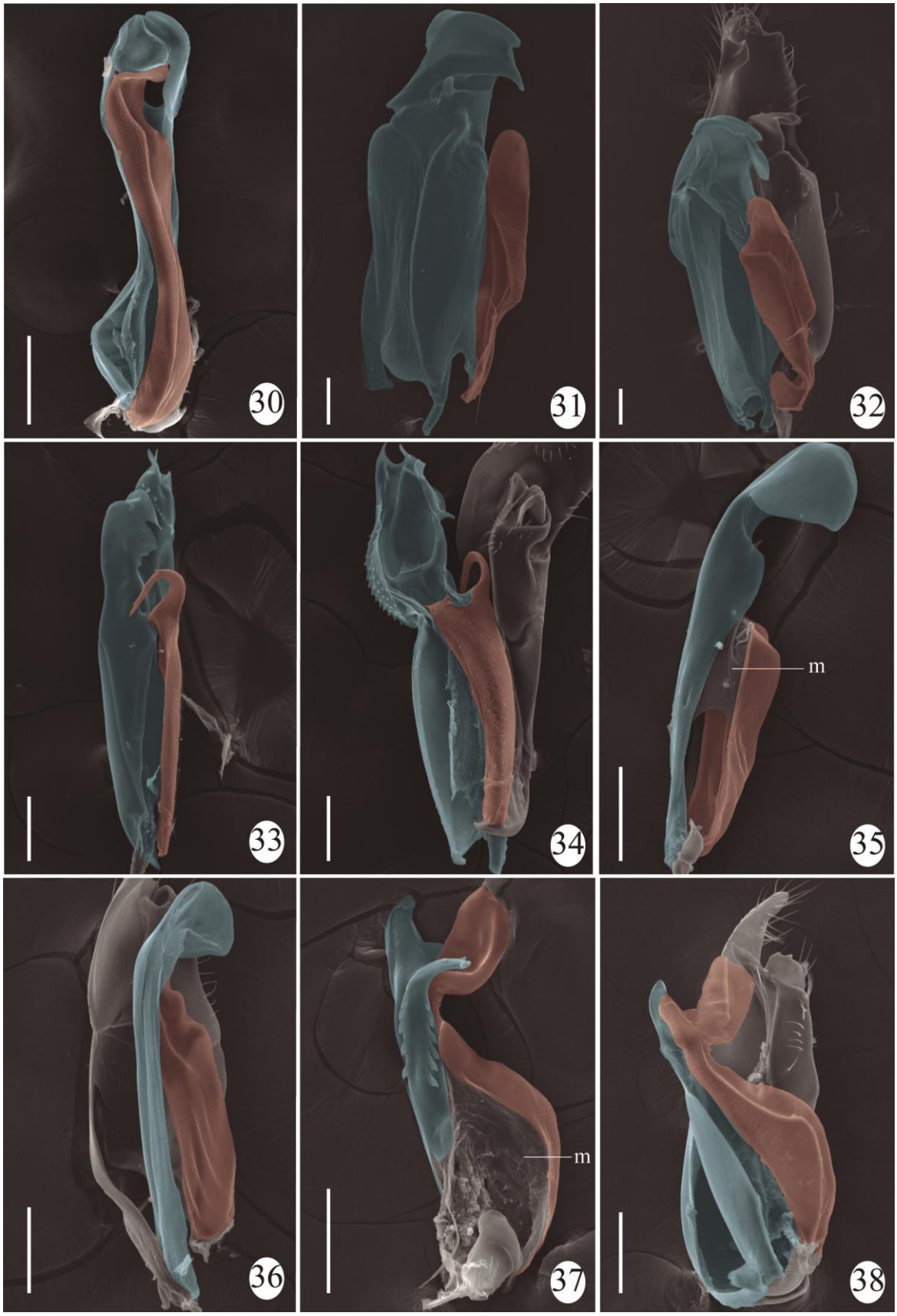

Figures 30–**38.** Male genitalia, lateral view of complex aedeagus. 30. Genus D, internal lateral face. 31–32. *Pristocera*. 31. External lateral face. 32. Internal lateral face. 33–34. *Propristocera*. 33. External lateral face. 34. Internal lateral face. 35-36. *Protisobrachium*. 35. External lateral face. 36. Internal lateral face. 37–38. *Trichiscus*. 37. External lateral face. 38. Internal lateral face. Dorsal body colored in blue, ventral ramus in red. Scale bar: 100 µm.

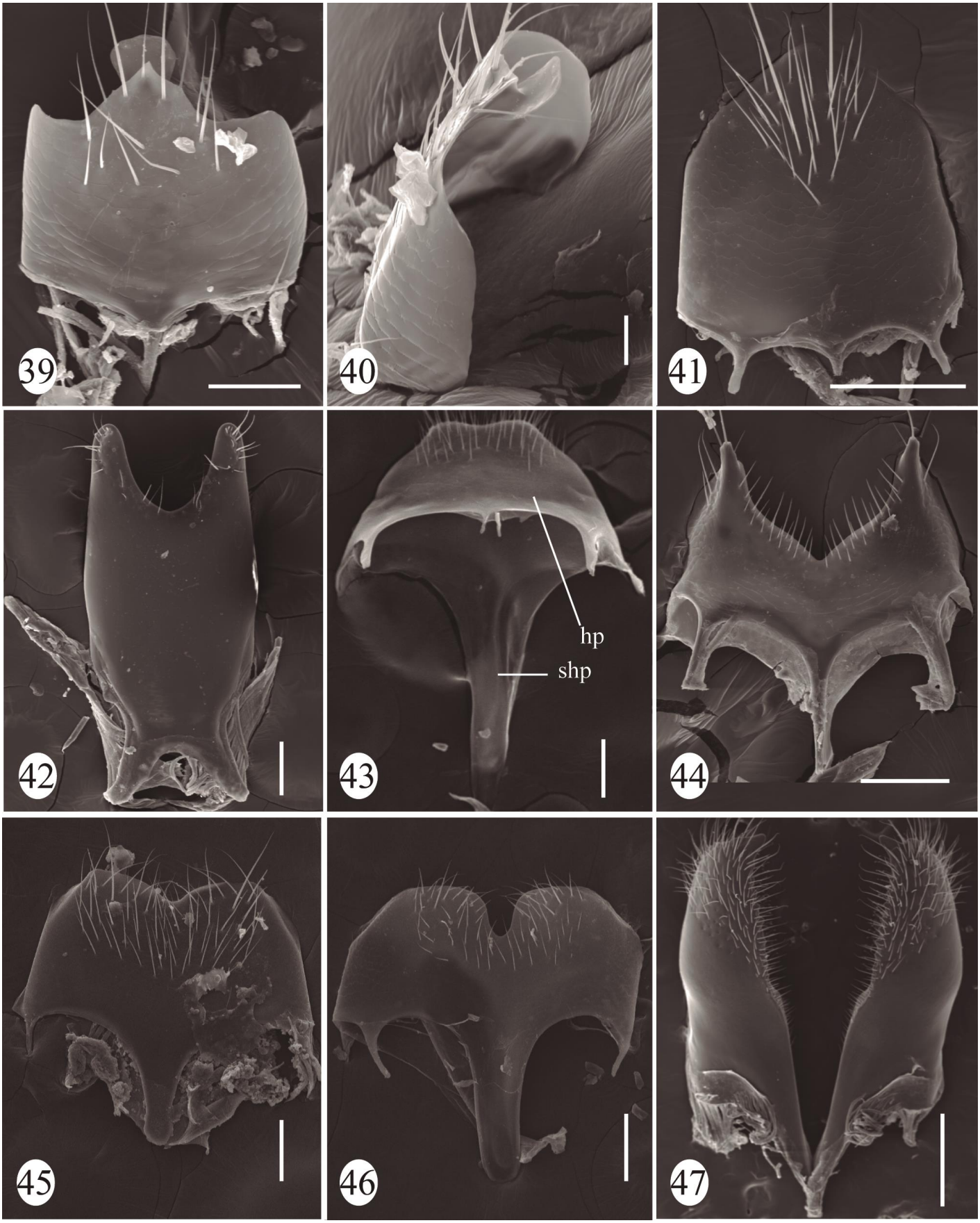

Figures 39–47. Hypopygium in dorsal view. 39–40. *Calobrachium*. 40. Ventral posterior projection dropshaped. 41. *Pseudisobrachium*. 42. *Zimancus*. 43. *Apenesia*. 44. *Foenobethylus*. 45. Genus B. 46. *Trichiscus*. 47. *Pristocera*. Label: (hp) hypopygeal plate; (shp) subhypopygeal plate. Scale bar: 100 µm, except 39 (50 µm), 40 (20 µm) and 47 (50 µm).

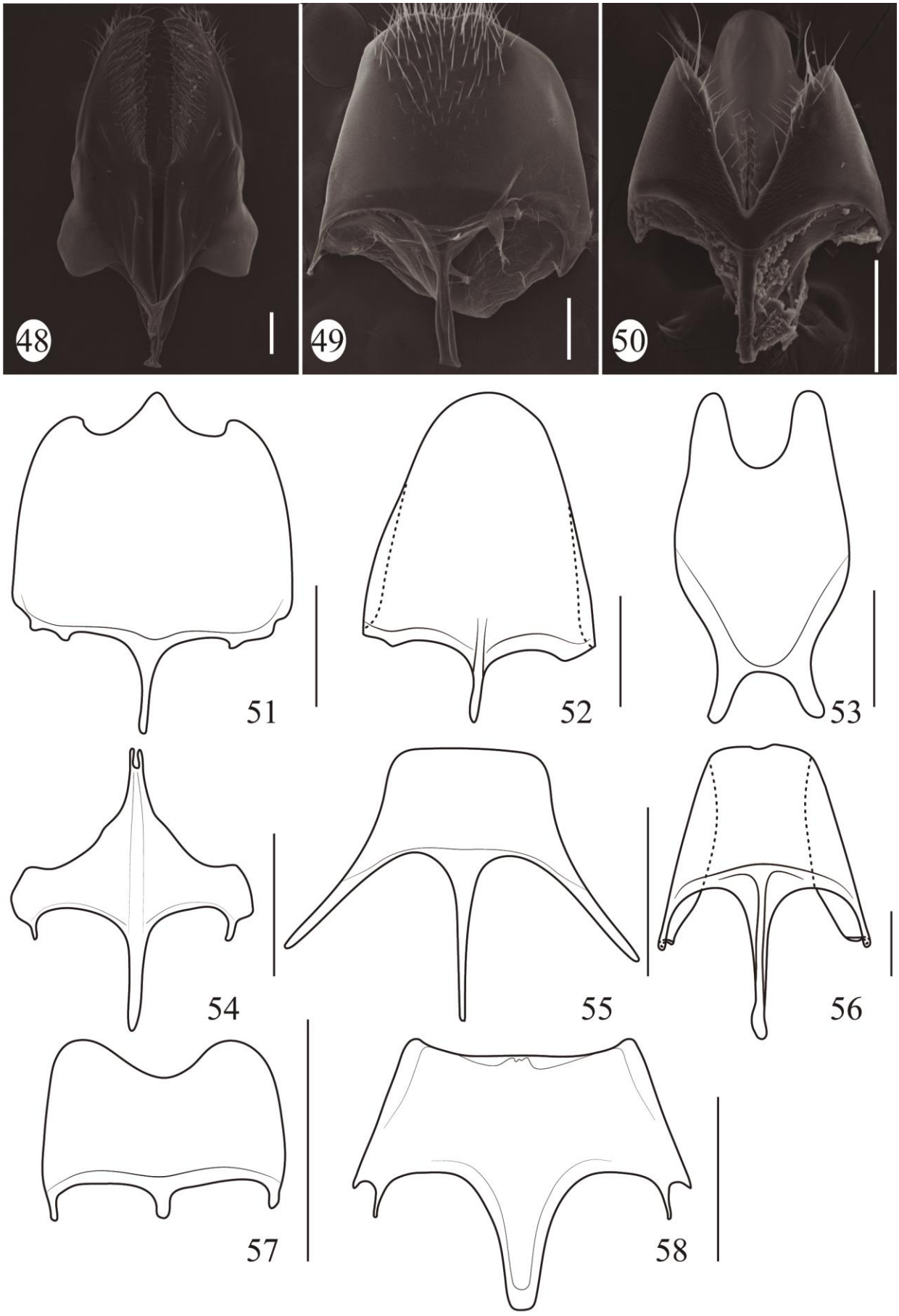

Figures 48–**58.** Hypopygium in dorsal view, except 48, ventral view. 48. *Pristocera*. 49. *Pristepyris*. 50. *Propristocera*. 51. *Caloapenesia*. 52. Genus A. 53. *Heterocoelia*. 54. *Eupsenella*. 55. *Paraceleroderma*. 56. Genus D. 57. *Protisobrachium*. 58. *Dissomphalus*. Scale bar: 48–50, 200 µm, 51–28, 250 µm.